The Role of Global Datasets for Flood Risk Management at National Scales

Mark V. Bernhofen[1], Sarah Cooper[1], Mark A. Trigg[1], Anna Mdee[1], Andrew Benedict Carr[1], Ajay Gajanan Bhave[2], Yady Tatiana Solano-Correa[3], Edgar Leonairo Pencue-Fierro[3], Ermias Teferi[4], Alemseged Tamiru Haile[5], Zulkifli Yusop[6], Nor Eliza Alias[6], Zulfaqar Sa'adi[6], Muhamad Anwar Bin Ramzan[6], C T Dhanya[7], and Prabhakar Shukla[7]

[1]University of Leeds
[2]University of Newcastle
[3]University of Cauca
[4]Water and Land Resource Center
[5]International Water Management Institute
[6]Universiti Teknologi Malaysia
[7]Indian Institute of Technology Delhi

November 22, 2022

Abstract

Over the last two decades, several datasets have been developed to assess flood risk at the global scale. In recent years, some of these datasets have become detailed enough to be informative at national scales. The use of these datasets nationally could have enormous benefits in areas lacking existing flood risk information and allow better flood management decisions and disaster response. In this study, we evaluate the usefulness of global data for assessing flood risk in five countries: Colombia, England, Ethiopia, India, and Malaysia. National flood risk assessments are carried out for each of the five countries using global datasets and methodologies. We also conduct interviews with key water experts in each country to explore what capacity there is to use these global datasets nationally. To assess national flood risk, we use 6 datasets of global flood hazard, 7 datasets of global population, and 3 different methods for calculating vulnerability that have been used in previous global studies of flood risk. We find that the datasets differ substantially at the national level, and this is reflected in the national flood risk estimates. While some global datasets could be of significant value for national flood risk management, others are either not detailed enough, or too outdated to be relevant at this scale. For the relevant global datasets to be used most effectively for national flood risk management, a country needs a functioning, institutional framework with capability to support their use and implementation.

Hosted file

`supporting_information.docx` available at https://authorea.com/users/540796/articles/600334-the-role-of-global-datasets-for-flood-risk-management-at-national-scales

Hosted file

`essoar.10508948.1.docx` available at https://authorea.com/users/540796/articles/600334-the-role-of-global-datasets-for-flood-risk-management-at-national-scales

Mark V Bernhofen[1], Sarah Cooper[2], Mark Trigg[1], Anna Mdee[2], Andrew Carr[1], Ajay Bhave[3], Yady Tatiana Solano-Correa[4], Edgar Leonairo Pencue-Fierro[4], Ermias Teferi[5,6], Alemseged Tamiru Haile[7], Zulkifli Yusop[8], Nor Eliza Alias[8,9], Zulfaqar Sa'adi[8], Muhamad Anwar Bin Ramzan[8], C. T. Dhanya[10], Prabhakar Shukla[10]

[1] School of Civil Engineering, University of Leeds, Leeds, LS2 9JT, United Kingdom

[2] School of Politics and International Studies, University of Leeds, Leeds, LS2 9JT, United Kingdom

[3] School of Engineering, Newcastle University, Newcastle, NE1 7RU, United Kingdom

[4] Grupo de Estudios Ambientales, University of Cauca, Calle 5 #4-70, 190003 Popayán, Cauca, Colombia.

[5] Water and Land Resource Center, P.O. Box 3880, Addis Ababa, Ethiopia

[6] Center for Environment and Development, Addis Ababa University, P.O. Box 1176, Addis Ababa, Ethiopia

[7] International Water Management Institute (IWMI), P.O. Box 5689, Addis Ababa, Ethiopia

[8] Centre of Environmental Sustainability and Water Security, Universiti Teknologi Malaysia, Skudai, 81310 Johor Bharu, Malaysia

[9] Department of Water and Environmental Engineering, School of Civil Engineering, Faculty of Engineering, Universiti Teknologi Malaysia, Johor Bahru 81310, Malaysia

[10] Department of Civil Engineering, Indian Institute of Technology (IIT) Delhi, New Delhi, India

Key Points

- 16 different global datasets are used to calculate national flood risk in Colombia, England, Ethiopia, India, and Malaysia.

- Flood risk estimates differ substantially at the national level and some datasets are not appropriate for use at the national scale.

- The capability of regional and local governance in interpreting and using global data is addressed.

Abstract

Over the last two decades, several datasets have been developed to assess flood risk at the global scale. In recent years, some of these datasets have become detailed enough to be informative at national scales. The use of these datasets nationally could have enormous benefits in areas lacking existing flood risk information and allow better flood management decisions and disaster response.

1

In this study, we evaluate the usefulness of global data for assessing flood risk in five countries: Colombia, England, Ethiopia, India, and Malaysia. National flood risk assessments are carried out for each of the five countries using global datasets and methodologies. We also conduct interviews with key water experts in each country to explore what capacity there is to use these global datasets nationally. To assess national flood risk, we use 6 datasets of global flood hazard, 7 datasets of global population, and 3 different methods for calculating vulnerability that have been used in previous global studies of flood risk. We find that the datasets differ substantially at the national level, and this is reflected in the national flood risk estimates. While some global datasets could be of significant value for national flood risk management, others are either not detailed enough, or too outdated to be relevant at this scale. For the relevant global datasets to be used most effectively for national flood risk management, a country needs a functioning, institutional framework with capability to support their use and implementation.

Keywords

Floods, Exposure, Vulnerability, Risk, Disaster risk analysis and assessment

1 Introduction

Flooding is a global problem that affects most regions in the world. In the last twenty years, over 1.65 Billion people were affected by flooding (UNDRR, 2020), while estimated losses as a result of flood events exceeded 1 Trillion US Dollars over the last forty years (MunichRE). The impacts of flooding can be reduced through good flood risk management (FRM). For FRM measures to be most effective, they need to be implemented in areas of high flood risk, which are identified through flood risk assessments. These assessments follow the conceptual framework that flood risk is a product of hazard (the flooding), exposure (who or what is exposed to the flooding), and vulnerability (the susceptibility of the exposure to damages) (UNISDR, 2015).

The objectives and data required for flood risk assessments change with the spatial scale of the analysis (de Moel et al., 2015). At the city or basin scale, flood risk assessments are carried out using locally calibrated models and data. The results of assessments at this scale are used to inform local flood management strategies and the design of flood mitigation infrastructure. National scale flood risk assessments either combine regionally derived flood information into a national picture of flood risk, such as with the National Flood Insurance Program (NFIP) in the US (Burby, 2001) and the National Flood Risk Assessment (NaFRA) in the UK (Environment Agency, 2009), or risk is mapped nationally in its entirety (Hall et al., 2003, Hall et al., 2005). The objectives of national flood risk assessments are to inform joined up strategic FRM, allowing for prioritized evidence-based interventions. They also provide nationally consistent data for planning. For flood risk assessments at these scales, there is a bias in the evidence base towards contexts with greater research and monitoring capability. Since the mid-2000s, efforts have been made to assess flood risk at the global

scale using globally available data (Hall, 2014, Ward et al., 2020a). Global flood risk assessments are a multi-national equivalent of the national approach. International agencies and stakeholders want consistent data and approaches to make strategic investments at the global scale. Early global assessments used simple coarse resolution flood risk data, necessary at the time to assess flood risk at such large spatial scales (Dilley et al., 2005, Hirabayashi et al., 2008). Recent advances in global flood risk data, both in resolution and accuracy, have expanded their potential usefulness beyond global studies of flood risk to include more local applications, filling data gaps that had previously precluded flood risk assessments in data and institutional capability constrained regions. Some global data is now detailed enough to be relevant at national and catchment scales. This could, in theory, have potential benefits in areas lacking existing flood risk information and allow better flood management decisions and disaster response. Whilst the list of global datasets is large and growing (Lindersson et al., 2020), not all global datasets are created equally. There is an urgent need to evaluate available global flood risk datasets for use at the national scale.

There are two approaches to representing flood hazard globally: either through remote sensing (RS) of historical flood events or through global flood models (GFMs). The two are often considered complimentary (Hawker et al., 2020), as RS data is used to validate the global models (Bernhofen et al., 2018, Mester et al., 2021). GFMs use global datasets, automated methods, and simplified hydraulic equations to simulate flood hazard globally (Trigg et al., 2020). These models, which began as research experiments, are now being used for disaster response (Emerton et al., 2020), to inform policy decisions (Ward et al., 2015), to assess business risks (Ward et al., 2020b), and recently their modelling frameworks have incorporated detailed national level data to assess national flood risk (Wing et al., 2017, Wing et al., 2018, Bates et al., 2021). Several GFMs have been developed in academia (Yamazaki et al., 2011, Ward et al., 2013), by research institutions (Dottori et al., 2016, Rudari et al., 2015), and by commercial companies (Sampson et al., 2015). Their differing approaches to global flood hazard mapping result in flood extent disagreement (Trigg et al., 2016, Aerts et al., 2020) and varied performance (Bernhofen et al., 2018), suggesting no single model is uniformly fit for purpose.

Similarly, global population maps, necessary for calculating exposure, adopt equally divergent approaches to mapping human population. These range in complexity from simply distributing census data across administrative boundaries to statistically estimating population distribution and density from auxiliary datasets that relate to human presence (Leyk et al., 2019). Recent studies by Smith et al. (2019) and Bernhofen et al. (2021) found that flood exposure estimates are significantly impacted by the population dataset used. As these datasets become increasingly locally relevant, there is an urgent need to investigate their fitness-for-use in flood risk assessments at these scales.

A key component of flood risk assessments, frequently absent from global studies, is vulnerability (Ward et al., 2020a). Vulnerability is multifaceted; it can

be assessed through societal, economic, environmental, or physical means (Birkmann et al., 2006). The most visible, and most commonly assessed, aspect of vulnerability is direct damages (Meyer et al., 2013). Direct damages are typically calculated using some form of vulnerability curve, which translates a component of the modelled flood hazard (often depth) into a degree of damage. Depth-damage curves are derived from data collected from historical flood events or expert judgement; or a combination of the two (van Westen, 2014). As a result, vulnerability functions are globally disparate. In countries with a wealth of historical data, such as the UK (Penning-Rowsell et al., 2013), the Netherlands (Kok, 2004), and the US (Davis and Skaggs, 1992) there are detailed vulnerability functions, whereas in other countries there are none at all. These data gaps were addressed by Huizinga et al. (2017) who developed a global database of depth-damage functions for multiple land-use classes. Significant uncertainties remain, however, both in the datasets used to identify assets at risk in the vulnerability calculations and in the assumptions made about the land-use classes.

A cross-disciplinary approach needs to be taken when evaluating global datasets for FRM at national scales (Morrison et al., 2018). The physical science (global data) needs to be understood in the context of the social science. There needs to be a focus on the capabilities of regional and local governance in interpreting and using this data to inform and address flood risk. Governing bodies require datasets to be accessible, unambiguous, and easy to use; however, variability between datasets poses risks for effective policy and decision-making, for example the different conceptualizations of vulnerability may not translate to actual administrative and political structures. Also integral is the capacity of organizations and other governance structures to use the data. Human, technical, and financial resources of services are often lacking. Failures in coordination and communication between related departments and other relevant stakeholders over other scales may result in the incorrect use of data. For example, the dissemination of data to the local scale can be complicated and challenged by local priorities, alternative perceptions, elite capture, and language. Data also has the potential to be manipulated and/or abused in power struggles or for political motives (Wissman-Weber and Levy, 2018, Venot et al., 2021).

The UKRI GCRF Water Security and Sustainable Development Hub project (https://www.watersecurityhub.org/) connects water experts in five different countries, spanning four continents. This project provides a unique opportunity to test the global datasets for use at these scales in countries with vastly different histories of flooding and flood management structures and allows us to explore the commonality and variability of global data used locally. In this paper, we use global datasets and methods from previously published studies of global flood risk to carry out flood risk assessments in five countries: Colombia, England, Ethiopia, India, and Malaysia. We calculate national flood risk using a 20-year catalogue of historical flooding, five GFMs, seven global population datasets, and three approaches to calculating vulnerability. We then assess the credibility of this data for use at the national scale considering the variability of the flood

risk estimates and exploring the implications this has on their usefulness. We also examine the capacity to use this data for FRM in each country.

2 National flood risk management approaches, study countries, and the role of global data

2.1 National flood risk management approaches

There are two distinctive approaches to FRM, as laid out by Morrison et al. (2018): the resistance approach and the adaptive approach. The resistance, or standard, approach to FRM consists of mitigating flood risks through infrastructure or laws and regulations. The adaptive approach focusses less on preventing flooding and places greater emphasis on increasing resilience in high risk areas (Schelfaut et al., 2011). The approaches are complimentary, and successful examples of FRM often consist of a marriage of the two (van Wesenbeeck et al., 2014).

The implementation of FRM strategies typically falls on the government. The level of government responsible for executing FRM strategies is dependent on the country and the strategy being implemented (Merz et al., 2010). Governance strategies to FRM vary, as countries prioritize certain approaches over others (Driessen et al., 2018). Governance strategies can be hierarchical, consisting of a traditional 'top down' decision making structure (Alexander et al., 2016a); they can be decentralized, where policy decisions are made at the local level with a greater emphasis placed on stakeholder engagement (Driessen et al., 2012); they can be polycentric, where policy power is shared between different levels of government and non-government stakeholders (Loeschner et al., 2019, Garvey and Paavola, 2021); or they can be panarchy, which is an adaptive approach to governance that consists of a nested set of adaptive cycles (Gunderson and S, 2002, Alexander et al., 2016a), where certain conditions can trigger 'bottom up' changes in the system (Garmestani and Benson, 2013).

To evaluate global flood risk data for use at the national scale it is important to understand a country's approach to national FRM. Where, and how, the data will be used will depend on the national FRM strategy and who is responsible for implementing it. Taking a multi-country approach, as we are doing, enables us to pick apart the differences and commonalities in national strategies and how these influence the applicability of global flood risk data in a national flood risk context.

2.2 Study Countries

We evaluate the global data for use at the national level in five countries: Colombia, England, Ethiopia, India, and Malaysia. These five countries bring together local communities and 46 different stakeholder partners that work together to address water security issues in the Global Challenges Research Fund (GCRF) funded Water Security and Sustainable Development Hub (https://www.watersecurityhub.org/). Below, we briefly summarize flood risk in each country and how it is managed.

2.2.1 Colombia

Colombia is particularly susceptible to extreme weather events such as hurricanes, storms, and flooding due to its hydro-climatology that emerges from Colombia being located in the Intertropical Convergence Zone (ITCZ). The ITCZ is a place where both warm and humid winds from Northern and Southern latitudes converge, creating a belt of clouds. This situation generates constant provision of wind and humidity that, when interacting with topography, defines the rainy and dry seasons. The hydro-climatology is further influenced by El Niño–Southern Oscillation (ENSO). The cold phase of ENSO, otherwise known as La Niña, increases rainfall which leads to increased river flow and flooding. For example, in 2011 four million people were affected by a strong La Niña event, causing losses of $7.8 billion through damage to economic infrastructure, flooding of agricultural land, and the issuing of government subsidies (Hoyos et al., 2013). Climate change is also projected to increase rainfall by 2.5% by 2050 which will further increase incidences of flooding (Ramirez-Villegas et al., 2012). Colombia manages flood risk alongside other risks posed by volcanos, landslides, and earthquakes under their National Disaster Risk Management System (UNGRD in Spanish). Policy, legislation, and regulations under this system are decentralized over the global, national, regional, and local levels to directly include public entities, non-profit entities and communities within the policy's remit and subsequent activities. Colombia takes an ex-post approach to FRM through a reaction to flood events which occur.

2.2.2 England

Flooding has been recognized by the UK government as one of the most serious threats facing the country. The National Flood Risk Assessment (NaFRA) estimate that one in six commercial and residential properties are at risk from surface water, fluvial, and coastal flooding. These risks are exacerbated by factors such as population growth, deteriorating drainage infrastructure, land use change and natural erosive processes, and will worsen with climate change (Alexander et al., 2016b). Extreme flood events have become more frequent in recent years, for example, Kendon et al. (2019) report that in 2019 England and Wales had its fifth wettest autumn since 1766 resulting in severe flooding in Yorkshire, Nottinghamshire, Derbyshire, and Lincolnshire; the most severe flood event to occur in the UK since 2015. Governed by the Department for Environment, Food and Rural Affairs (DEFRA), current flood risk policy centers on resilience to manage flood and climate change risk and to protect economic growth and infrastructure. It recognizes the importance of public participation over a decentralized structure to nurture long term and flexible approaches; to enable life to continue alongside water rather than keeping water out (Forrest et al., 2017). This entails community groups working alongside other flood related agencies to come up with long term solutions.

2.2.3 Ethiopia

Ethiopia is exposed to a wide range of disasters associated with the country's

diverse geo-climatic and socio-economic conditions, but floods and droughts represent major challenges to communities and livelihoods. Flooding has become one of the most common, frequent, and severe natural disasters in Ethiopia affecting lowlands, highland, and urban areas; displacing thousands and causing loss of property and livelihoods. Increased rainfall variability and extreme events have increased the likelihood of flooding, while risk is exacerbated by rapid population growth and urbanization, particularly in Addis Ababa the capital (Haile et al., 2013a, Beshir and Song, 2021). Environmental degradation, poverty and conflict further aggravate the risks and reduce the coping capacity and resilience of communities. For example, Haile et al. (2013b), illustrate how resettlement programs by the Ethiopian Government between 1983 and 1996 in the lowland region Gambela and consequent land use change resulted in increased flood events that affected up to a third of the population in some woredas. FRM in Ethiopia is governed by the National Disaster Risk Management Commission (NDRMC), established in 2015, to coordinate an integrated approach with all hazards to streamline their disaster risk management approach over multiple administrative scales to including an early warning and response system across all government sectors. The Government of Ethiopia (GOE) has a long institutional history of addressing disaster risk management (DRM), starting with the establishment of the Relief and Rehabilitation Commission (RRC) following the 1974 famines. Since then, the country has taken several steps to shift to a more proactive approach to DRM. This includes updating the National Policy and Strategy on DRM (2013) and developing a DRM Strategic Program and Investment Framework (SPIF) for government and donor interventions in 2014 (DRMFSS, 2014).

2.2.4 India

Flood risk in India differs across the country due to the various geomorphological locations and different atmospheric circulations. The Indian Summer Monsoon through several transient atmospheric conditions brings rain to different parts of the country via different monsoonal phases as onset and advance (mid-May to mid-July), peak rainfall (July to August) and withdrawal (mid-September to mid-October). Rainfall intensity and extreme flood events have increased in intensity between 1951 and 2015 (Vinnarasi and Dhanya, 2016, Ray et al., 2019). Flood risk is a particularly severe for urban settlements in India due to the huge populations who reside in mega-cities (population of over 1 million). The number of mega-cities has risen exponentially to 52 cities over the last two decades due to migration from rural areas (De et al., 2013). Flooding and water-logging have become common occurrences due to the reduction of green spaces and aging storm drains which struggle to cope, especially during the monsoon seasons, leading to loss of income and increased disease risk (Ali et al., 2021). In the capital, Delhi, 24,840 hectares of the city is built on floodplains, 68% of which are the low-lying Yamuna floodplains. The apex organization for flood management schemes of India is the Central Water Commission (CWC). However, FRM in India is always state-led, with the federal government only assisting when relief measures (e.g., through National Disaster Response Force (NDRF), State Disas-

ter Response Fund (SDRF) etc.) are required. Many States, especially the ones which are flood-prone, have established Flood Control Boards, organized by the respective Irrigation Departments (majorly), to assess the flood problems and evaluate the flood schemes. For example, the Irrigation and Flood Control Department leads FRM in Delhi. The city is demarcated into six drainage zones, and twelve municipal zones manage the storm run-off between them for the whole city. This approach reflects the structural approach of policy to flood risk which focuses on mainly infrastructural measures to control flooding. Different structural/administrative measures have been adopted by these organizations to reduce the flood losses and protect the flood plains across India. In addition to the several laws enacted by the Central Government (e.g., Inter-state River Disputes Act 1956, The River Boards Act of 1956, Damodar Valley Corporation Act, 1948, Betwa River Board Act, 1976, Brahmaputra Board Act, 1980, The Land Acquisition Act, 1894 etc.), a few States have also enacted laws to deal with disputes related to flood control works (CWC, 2018).

2.2.5 Malaysia

Malaysia is severely affected by flooding. Eighty-five of Malaysia's 189 river basins are prone to recurrent flooding, all of which flow into the South China Sea (Saifulsyahira et al., 2016). Rainfall intensity in Malaysia is high all year round, with most of the flooding occurring between November and February during the Northeast Monsoon. For example, in January 2021, six people died and 50,000 were displaced during the monsoon on the east coast (Al Jazeera, 2021). Flash floods have also become more common with increased urbanization, infrastructure development alongside rivers, and the poor maintenance of drains and waterways (Yusoff et al., 2018, Mabahwi et al., 2020). FRM in Malaysia is driven by the federal government and characterized by a mostly technocratic approach. The Department of Irrigation and Drainage Malaysia (DID) is the main entity involved with flood management which includes the management of hydrological data, planning and development of flood defenses, planning and development of flood mitigation, management of national river resources, and coordination of other relevant agencies over federal, state and district administrative levels (Mabahwi et al., 2020).

2.3 The role of global data

The use of global datasets to assess national flood risk is dependent on the extent to which countries have the capacity, institutions, and governance structures to use and interpret the information. Many countries, especially those in the Global South, frequently lack the resources, expertise and strong institutional frameworks needed to access, collect, interpret, and analyze available datasets to implement effective FRM. For example, in Colombia, the gap between policy, the political will, and capacity to act on flooding influences FRM; also the country's ex-post approach to FRM may limit the usefulness of these datasets (Key Informant Interview, Universidad del Valle, 2021). In Malaysia, efforts to manage flood disasters are hampered by a lack of legislative guidance on the management of flooding within the National Disaster Management Agency

(NADMA), the federal agency in charge of disaster risk management, despite the NADMA's close association with flooding management agencies. Obstructive bureaucracy over administrative scales and between agencies and limited authority in decision making also restrains the ability to manage flood risk in Malaysia (Mabahwi et al., 2020). Effective use of global flood risk data by these countries also entails corroboration with local data collected concerning flood risk, however local data may be limited, unavailable, or incompatible with global datasets due to poor data management, lack of resources systems, and unreserved, restricted access to data.

3 Global Data

The number of global datasets for calculating climate risks is large and growing (Lindersson et al., 2020). In this study, we use global datasets that have been used in previously published studies of global flood risk. The datasets we use are free and can be easily obtained by the end-user, either by directly downloading them online or by contacting the developer of the datasets. In total, we use 6 global datasets of flood hazard, 7 global datasets of human population, and 3 global approaches to calculating vulnerability. These datasets are detailed in the sections below and in *Tables 1* and *2.*

3.1 Global Flood Hazard Data

We use both models and satellite observed flood events to represent hazard. We use five GFMs that have been used in previous studies of global flood risk. The models are CaMa-UT (Zhou et al., 2020, Yamazaki et al., 2011), CIMA-UNEP (Rudari et al., 2015), Fathom (Sampson et al., 2015), GLOFRIS (Ward et al., 2020b, Ward et al., 2013, Winsemius et al., 2013), and JRC (Dottori et al., 2016) These models represent the state-of-the-art in publicly available global flood hazard maps. They produce spatially continuous flood maps, meaning that the return period simulated is assumed constant across the modelled domain. The five models can be categorized into two distinct structures: cascade model structure and gauged flow data model structure (Trigg et al., 2016). Cascade models use global climate precipitation data to force land surface models which predict extreme flows across the river network. Gauged flow data models use global gauge data and regional flood frequency analysis to estimate extreme flows in ungauged basins globally. Previous intercomparison studies found large differences between these models in Africa (Trigg et al., 2016) and China (Aerts et al., 2020). Validation of the same models against observed flooding in Nigeria and Mozambique found that the best models performed favorably compared with historical flood events (Bernhofen et al., 2018). Some, but not all, of the GFMs have incorporated flood defenses into their modelling frameworks. Similarly, some models have introduced different types of flooding, such as pluvial and coastal. To maintain consistency between the GFMs we use only the fluvial undefended flood hazard maps. The 100-year return period, or 1% annual probability flood, is used for our calculations. In England, we use Fathom-UK flood extents, which utilizes the same modelling framework as their global model but makes use of more detailed national data. In addition to globally modelled flood

9

extents, we use satellite derived flood extents from the Global Flood Database (GFD), a 20-year catalogue of observed flood events (Tellman et al., 2021). The global flood hazard datasets are outlined in *Table 1*. Detailed descriptions of the datasets and how to access them, as well as previous flood risk studies they have been used in are included in the Supplementary Material.

Table 1. Global Flood Hazard Data Summary Table

Flood Models

Name	Model Structure	Rivers Modelled	Inundation Solver	Elevation Data	Downscaling Procedure	Output Resolution
CaMa-UT	Cascade	Catchments > 0.25° grid cell (~600 km^2) some inundation captured on rivers as small as 50 km^2 during downscaling	2D inertial wave	SRTM (MERIT)	Flood depth downscaled from 0.25 degrees	arcsecond
CIMA-UNEP	Gauged flow	Rivers > 1000 km^2 drainage area	1D manning's	SRTM (HydroSHEDS)	None	arcsecond
Fathom Global 2.0	Gauged flow	Rivers > 50 km^2 drainage area	2D inertial wave	SRTM (MERIT)	None	arcsecond
Fathom-UK		All rivers		LiDAR		arcsecond
GLOFRIS	Cascade	Rivers Strahler order 6	2D kinematic wave	SRTM (HydroSHEDS)	Volume redistributed from 0.5 degrees	arcsecond

Flood Models						
JRC	Cascade	Rivers > 5000 km² drainage area	2D inertial wave	SRTM (HydroSHEDS)	None	arcsecond
Observed Data						
Name	**Image Source**	**Type of Flooding**	**Image Type**	**Observed Period**	**Total Events**	**Resolution**
Global Flood Database (GFD)	MODIS	Heavy rain, Storm surge, Snowmelt, Dam break,	Optical	-2018		m

3.2 Global Population Data

To identify who is exposed to flooding it is essential to understand where people live. Gridded population datasets, which distribute census information over spatial data, are the tools commonly used to calculate flood exposure at the global scale. The methods applied to distribute census data differ in complexity. These methods, their development, and their wide-ranging applications are reviewed in detail by Leyk et al. (2019). To summarize the different methods briefly, census data can be distributed across a grid by areal weighting or by dasymetric weighting. The areal weighting approach distributes census data evenly across an area. The dasymetric weighting approach uses ancillary datasets to weight the distribution of census data. This can vary in complexity from binary weighting (settlement or no settlement) to statistical weighting approaches based on multiple ancillary datasets. Another way to distinguish the population datasets is whether they are constrained or unconstrained. The constrained approach masks out all non-settled areas as uninhabited, while the unconstrained approach assumes that not all settlements can be accurately mapped globally and residual census data is distributed across non-settled area to account for any unmapped settlements (Thomson et al., 2021)

The use, and limitations, of gridded population data in flood exposure studies specifically, are addressed in the studies of Smith et al. (2019) and Bernhofen et al. (2021). The two studies collectively consider four different global population datasets, however, many more have been used in previous studies of global

flood risk. In *Table 2*, we identify and summarize seven different global population which we use to calculate flood exposure: GPW4 (Doxsey-Whitfield et al., 2015), GHS-POP (Freire et al., 2016), GRUMP (Balk et al., 2005), HRSL (Tiecke, 2017), HYDE (Klein Goldewijk et al., 2010, Klein Goldewijk et al., 2017), Landscan, and Worldpop (Stevens et al., 2015). These datasets have all been used in previous studies of global flood risk. In our analysis, we use the most up-to-date epoch for each population dataset, which are then scaled to 2020 national population totals for exposure comparison. Detailed descriptions of each population datasets and how to access them, as well as previous global flood risk studies they have been used in are included in the Supplementary Material.

Table 2. Global Population Data Summary Table

Name	Census Data	Daytime / Nighttime	Ye
GPW4	subnational census data (and UNDP adjustments)	Nighttime	200
GHS-POP	GPW4	Nighttime	197
GRUMP	GPW3	Nighttime	199
HRSL	GPW4	Nighttime	201
HYDE	UN world prospects and literature (pre-1950)	Nighttime	10,
Landscan	subnational census data (and U.S. Census Bureau adjustments)	Daytime	An
WorldPop	GPW4	Nighttime	An

3.3 Global Vulnerability Approaches

Vulnerability is the susceptibility of a community or system to experience losses from a hazardous event (UNISDR, 2004). It is a complex, multifaceted concept that can be experienced directly or indirectly across human, physical, economic, and environmental spheres (van Westen, 2014). Vulnerability has received less attention at the global scale than hazard and exposure (Ward et al., 2020a). Below, we identify and summarize three intercomparable methods for calculating vulnerability that have been used in previous studies of global flood risk. The three methods calculate direct economic damages using land cover maps to identify assets at risk and depth-damage curves to determine the degree of damage experienced by the asset. We name the three vulnerability approaches based on the global land cover map used to represent assets at risk.

3.3.1 GHSL

The approach to calculating vulnerability in the Aqueduct Floods project (Ward et al., 2020b) is based on the global depth-damage function database developed by Huizinga et al. (2017). Only urban damages are considered. The urban area is split into three classes: residential, commercial, and industrial. Because current global land cover datasets do not differentiate between urban classes, assumptions are made about the fractional split of urban classes globally. Based on the spatial distribution of urban classes in Europe derived from the Corine

Land Cover dataset and the findings of a report by the Buildings Performance Institute Europe (Economidou et al., 2011) the global fractional split of urban areas used in Ward et al. (2020b) is 75 percent residential, 15 percent commercial, and 10 percent industrial. Urban areas are defined as cells in the 1 km resolution Global Human Settlement Layer (GHSL) dataset (Corbane et al., 2019) that correspond to a percentage of built-up area of 50 percent or greater (Ward et al., 2020b).

3.3.2 GlobCover

The same global depth-damage function database (Huizinga et al., 2017) was used alongside the 10 arcsecond resolution (~300 m at the equator) GlobCover (v2.3) land cover map (Bontemps et al., 2011) to calculate vulnerability in a number of other studies of global flood risk (Alfieri et al., 2017, Alfieri et al., 2018, Dottori et al., 2018). In these studies, five land use classes were considered in the vulnerability assessment: four urban classes (residential, commercial, industrial, and infrastructure) and agriculture. This is the only approach of the three that considers any non-urban (agricultural) damages. While the GlobCover dataset explicitly represents agriculture area, it makes no distinction between urban land-use classes, which are represented as 'artificial areas'. These 'artificial areas' are split into the four urban land-use classes using globally consistent ratios, derived from studies of land-use occupation in cities across different continents (Dottori et al., 2018). The urban land-use ratios used are 56 percent residential, 20 percent commercial, 16 percent industrial, and 8 percent infrastructure (L. Alfieri, personal communication, December 1, 2020).

3.3.3 HYDE

In Ward et al. (2013) a single depth damage function, derived by averaging the high and low urban density land class functions in the Damagescanner tool (Klijn et al., 2007), is used to calculate vulnerability globally. Maximum damage values are calculated for each country following the approach of Jongman et al. (2012) which uses a country's GDP to normalize maximum damages obtained from the Damagescanner tool. Damages are calculated exclusively for urban areas which are derived from the HYDE (Klein Goldewijk et al., 2010) fractional urban landcover dataset at 5 arcminute resolution (~10 km at the equator). It should be noted that the limitations of using a single depth-damage function globally are outlined in Ward et al. (2013) and subsequent studies have incorporated spatially variable functions (Ward et al., 2020b).

4 Methods

4.1 GFM and Population Agreement Calculations

The datasets are aggregated following the approach of Trigg et al. (2016) and Aerts et al. (2020). GFM output is aggregated by first resampling the five GFMs to the finest GFM resolution (1 arcsecond in England and 3 arcsecond in the remaining countries) using the nearest-neighbor approach, which ensures depths of the resampled flood map are the same as the native resolution flood

map. The GFM flood depth maps are converted to binary wet/dry rasters for any non-zero flood depth and then summed to produce the aggregated GFM map. Permanent water bodies are masked out using the G3WBM permanent water body mask (Yamazaki et al., 2015). Values in the aggregated GFM map range from 5 (highest agreement) to 1 (lowest agreement). Similarly, to produce the aggregated population map the seven global population datasets are resampled to the finest population resolution (1 arcsecond). The population maps are then converted to binary populated area maps where any cell with a non-zero population is defined as a populated cell. It should be noted that this approach just represents the agreement between the population data in terms of populated area and does not account for variations in population density. Values in the aggregated population map range from 7 (highest agreement) to 1 (lowest agreement).

Agreement between the datasets is calculated using the Model Agreement Index (MAI) first introduced by Trigg et al. (2016) and three variations of this index. The MAI is calculated using the aggregated GFM map. For each model agreement level, the total flooded area is multiplied by the fractional level of agreement. These values are summed for all agreement levels and then divided by the total flooded area to give a fraction of model agreement, which ranges from 0 (no agreement) to 1 (total agreement).

$$MAI = \frac{\sum_{i=2}^{n} \frac{i}{n} \bullet a_{\mathrm{fi}}}{A_f} \quad (1)$$

where A_f is the total flooded area in the aggregated GFM map, i is the agreement level, n is the total number of models, and a_{fi} is the flooded area at the agreement level i. The Population Agreement Index (PAI) is calculated in the same way that the MAI is calculated. The only difference is that the aggregated population map rather than the aggregated GFM map is used in the calculations.

$$PAI = \frac{\sum_{i=2}^{n} \frac{i}{n} \bullet a_{\mathrm{pi}}}{A_p} \quad (2)$$

where A_p is the total populated area in the aggregated population map and a_{pi} is the total populated area at agreement level i. Values for the PAI range from 0 (no populated area agreement) to 1 (total populated area agreement). The Exposure Agreement Index (EAI) is another variation of the MAI. Similar to the exposure weighted metrics used in Pappenberger et al. (2007) and Wing et al. (2019), the EAI uses exposed population, rather than flooded area, to calculate agreement. EAI is calculated for each of the seven population datasets.

$$EAI = \frac{\sum_{i=2}^{n} \frac{i}{n} \bullet e_i}{E} \quad (3)$$

where E is the total population exposed to the entire aggregated GFM map and e_i is the population exposed at agreement level i. The EAI ranges from 0 (no model exposure agreement) to 1 (total model exposure agreement) and is an indicator of the level of agreement between the models when used for exposure calculations. The final agreement index is the Volume Agreement Index (VAI). While the MAI calculates agreement between the models in two dimensions, the VAI calculates model agreement in three dimensions by incorporating flood depth. The VAI needs to be calculated using the aggregated GFM map alongside all the GFM flood depth maps.

$$VAI = \frac{\sum_{i=2}^{n} \frac{i}{n} \bullet v_i}{V_{\max}} \quad (4)$$

where $V_{\max}$ is the maximum volume possible for the aggregated flood extent and v_i is the volume of models in agreement at agreement level i (in three dimensions). The VAI ranges from 0 (no agreement) to 1 (total agreement).

4.2 Flood Exposure Calculations

Flood exposure is calculated for each country using observational flood data, five GFMs, and seven population datasets outlined in *Section 3*. Observational flood data for the last 20 years is collated from the GFD and merged into one 20-year flood map. We remove any observed flood events caused by storm surges or by dams. In total, 237 events are merged across the five countries. There are two resolutions at which exposure calculations are carried out: 1 arcsecond and 3 arcsecond. Exposure calculations for the HRSL population map are carried out at 1 arcsecond resolution (the native resolution of HRSL). Similarly, in England exposure calculations are all carried out at 1 arcsecond resolution (the native resolution of the Fathom-UK flood map). The remaining exposure calculations are carried out at 3 arcsecond resolution. The six flood hazard datasets are resampled to 3 arcseconds resolution (if not already native at 3 arcseconds) and 1 arcsecond resolution using the nearest neighbor approach. Global population datasets coarser in resolution than 3 arcseconds (GHS-POP, GPW4, GRUMP, HYDE and LandScan) are resampled and the population is evenly distributed to a 3 arcsecond resolution grid (or 1 arcsecond in England). Flood exposure is calculated by intersecting a flood map with a global population dataset. Permanent water bodies are masked out using the G3WBM water body map (Yamazaki et al., 2015). To account for any differences in total national populations between the seven global population datasets (and because not all population data is in the same epoch), each dataset's total national population is scaled to match the WorldPop 2020 national population totals.

4.3 Flood Damage Calculations

Flood damages are calculated in each country using the five GFMs and three vulnerability methods outlined in Section 3. Observational data is not used for the vulnerability calculations as the maps contain no information about flood depth. Because the depth-damage curves are in units of metres, depths for the CIMA-UNEP GFM are first converted from centimetres to metres. Each vulnerability method uses a different landcover map (GlobCover, GHSL, and HYDE). These maps are resampled to the analysis resolution (1 arcsecond in England, 3 arcseconds in the rest) using the nearest neighbor approach. Permanent water bodies are masked out in the GFMs with the G3WBM water body map (Yamazaki et al., 2015)

For the GlobCover vulnerability method, the approach follows that of Alfieri et al. (2017) and Dottori et al. (2018). Damages are calculated across five different sectors: agriculture, commercial, industrial, infrastructure, and residential, the latter four making up the urban class. Those areas defined as "Artificial" in the GlobCover landcover map are classified as urban areas. Because the GlobCover map does not distinguish between urban sectors, we use constant urban ratios of 56% residential, 20% commercial, 16% industrial, and 8% infrastructure that have been used in the aforementioned studies. When defining agricultural areas, we use the GlobCover "Cropland" class. Where a range of potential cropland area is given in the GlobCover documentation we use the average value (e.g. for 20-50% coverage we use 35%). Damage curves and maximum damages for each sector in each country are taken from the Huizinga et al. (2017) global database of depth damage functions.

For the GHSL vulnerability method, we follow the Aqueduct approach (Ward et al., 2020b). Damages are calculated for three urban sectors: residential, commercial, and industrial. Urban areas are defined as those cells in the GHSL dataset with a built-up area greater than 50%. Constant ratios of 75% residential, 15% commercial, and 10% industrial are used for the urban sector split. The same Huizinga et al. (2017) database is used to determine maximum damage values and damage curves per sector in each country.

For the HYDE vulnerability method, we follow the approach outlined in Ward et al. (2013). Maximum damages for each country are calculated using a GDP normalization equation from Jongman et al. (2012) applied to a maximum damage value from the Damagescanner model (Klijn et al., 2007). To convert the maximum damage values from 2005 USD into 2010 EUR (to ensure consistency with the Huizinga et al. (2017) database), we use the average annual inflation from 2005 to 2010 and the average USD to EUR exchange rate for 2010. Urban areas are calculated using the HYDE urban land cover dataset for the year 2015, which shows the percentage urban coverage per grid cell. This percentage urban coverage is converted to an urban area, to which we assign the calculated country-specific maximum damage value. A single depth-damage function is used, which is the average of the functions for the high and low urban density classes in the Damagescanner model.

16

Damages are calculated for each of the three approaches by intersecting a GFM flood hazard map with depths with the relevant land use dataset. Where the flooding and the land use data intersect, percentage damage is calculated for the specific land use type using the flood depth at that location and the specific depth-damage curve for that sector. Damages are calculated by multiplying the percentage damage by the maximum damage value for that land-use type. Damages are reported in 2010 Euros.

4.4 Institutional Capacity of Flood Risk Management

Qualitative interviews are conducted among key water experts of the five countries to explore the extent and capacity to which they access and use these global datasets. Data from these interviews were used to illustrate the national context of FRM, as outlined in *Section 2*, and feed into the discussion in *Section 6*.

5 Results

5.1 Global Flood Hazard and Population Data Agreement

Aggregated maps of GFM hazard extent (*Figure 1*) were used to evaluate model agreement (see agreement scores in *Table 3*). In Colombia, the country with the best MAI score (0.363), the models showed the highest levels of agreement to the north of the country on the Magdalena river. In India, the country with the second highest MAI score (0.322), the areas of highest GFM agreement were in the north-east of the country, along the Ganges and the Brahmaputra rivers. This was a trend seen across the five countries: the models tended to agree more on larger rivers and disagree more on smaller rivers. This is evident in the Orinoquia region in central Colombia where only one of the five models predicts significant inundation. Most of the rivers here have an upstream drainage area less than 500 km^2. Of the five GFMs, Fathom is the only one that models rivers this small (rivers with an upstream drainage area greater than 50 km^2). The impact of river thresholds was most marked in England, here Fathom-UK has ingested higher accuracy national elevation and gauge data to model flooding on all rivers. By comparison, JRC only models flooding on six rivers in England. The models also disagree in low-lying coastal areas and deltas, such as the western Ganges delta and the Godavari delta in India, the Sarawak's Rajang River Delta in Malaysia, and the Fens
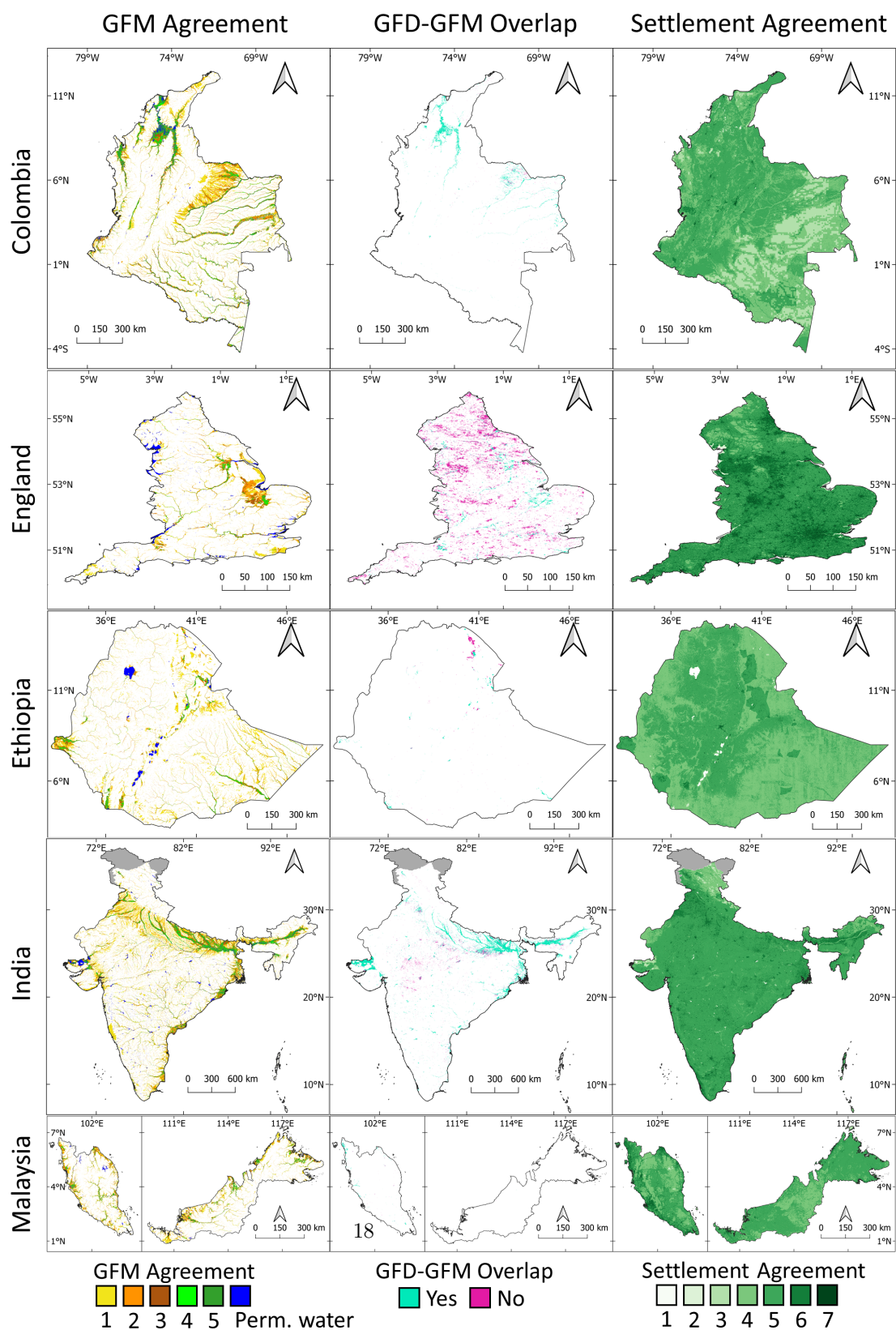

GFM Agreement   **GFD-GFM Overlap**   **Settlement Agreement**

Rows

Colombia

England

Ethiopia

India

Malaysia

Legends

GFM Agreement

1   2   3   4   5   Perm. water

GFD-GFM Overlap

Yes   No

Settlement Agreement

1   2   3   4   5   6   7

18

Figure 1. Maps of Global Flood Model (GFM) agreement, GFM and Global Flood Database (GFD) observed flooding overlap, and global population data settlement agreement. Grey areas indicate no-data regions.

in eastern England near The Wash. In these low-lying areas, the flood extent is more sensitive to differences in modelled flood depth leading to lower model agreement. To further disseminate model agreement, we split the countries into drainage basins from level 4 - level 6 according to the HydroAtlas (Linke et al., 2019) classification. Maps of basin level agreement scores can be found in the Supplementary Material. When examining the relationship in level 6 basins between the catchment area upstream of the basin and the MAI score within the basin, we found a positive normative association between the two (Spearman's rank coefficient, $= 0.429$), evidence that GFM agreement improves as the size of river modelled increases. Comparing MAI scores between coastal level 6 basins and inland level 6 basins we found that the mean inland MAI score (0.293) was 38% larger than the mean MAI score for coastal basins (0.212). The same trends were found when examining the relationships at basin levels 4 and 5 (results included in the Supplementary Material).

The preceding section considered agreement between the modelled flood extents in two dimensions. Agreement was also measured in three dimensions using the VAI score, which incorporates modelled flood depth in the calculation. In general, VAI scores showed similar trends to MAI scores: scores were higher in basins with larger rivers and lower in coastal basins compared to inland basins. At the national level, Colombia and India remained the two highest scoring countries with VAI scores of 0.217 and 0.183, respectively. Interestingly, Ethiopia had the third highest VAI score (0.169) despite having the lowest MAI score, suggesting there was greater agreement between the modelled flood depths in Ethiopia than in Malaysia or England.

To evaluate GFM agreement in a risk context, exposure agreement when intersected with a population map was calculated using the EAI score. EAI scores were calculated for each of the seven population maps (see *Table 3*). The lower a population map's EAI score the greater the proportion of exposure that falls within the low agreement zones of the aggregated flood map. As the EAI score decreases the effect the choice of GFM has on calculated flood exposure increases. For example, in Colombia the choice of GFM has a greater impact on exposure estimates calculated with Landscan (EAI of 0.232) than with HYDE (0.358). The implications of using different datasets for exposure calculations are explored in greater detail in *section 5.2*.

Comparing the maximum aggregated GFM extent with 20 years of observational flooding from GFD (see *Figure 1*) we find that in Colombia the GFMs capture over 92% of the historical flooding. Almost 40% of the captured flooding is in the high agreement zone of the aggregated map (5 models agree), likely because a large proportion of the observed flooding occurred in the north of the country where the models showed higher levels of agreement. In India, much of the observed flooding on the Ganges and Brahmaputra rivers is captured

by the models. However, there are large areas of observed flooding missed by the models in central India in the state of Madhya Pradesh. In England the 20-year observed flood extent (10,938 km^2) is almost as large as the maximum aggregated 100-year return period GFM flood extent (13,608 km^2), but with little overlap. Much of this observed flooding can be attributed to commission errors from cloud cover.

When assessing population map agreement, we consider only binary populated or unpopulated areas; we do not consider variations in population density. England's PAI score (0.782) (see *Table 3*) is much higher than the other four countries. This can also be seen visually in *Figure 1*, where the aggregated population map for England has more dark green areas relative to the other countries. Population disagreement stems largely from the differing approaches to modelling rural / low populated areas. Unconstrained population datasets (which spread residual census data across uninhabited areas) are responsible for the large areas of low population agreement in Colombia and Ethiopia in Figure 1 and contributes to their comparatively low PAI scores. Another contributing factor to population disagreement is the difference in dataset resolution. The finest (HRSL, 1 arcsecond) resolution dataset is detailed enough to identify individual buildings while the coarsest (HYDE, 5 arcminute) resolution dataset is detailed enough to identify only cities.

Table 3. Country level Model Agreement Index (MAI), Volume Agreement Index (VAI), Exposure Agreement Index (EAI), and Population Agreement Index (PAI) scores.

| Country | MAI | VAI | EAI | | | | | | | PA |
			GPW4	GHS-POP	GRUMP	HRSL	HYDE	LandScan	WorldPop	
Colombia	0.363	0.217	0.346	0.235	0.321	0.247	0.358	0.232	0.298	0.62
England	0.258	0.132	0.244	0.223	0.264	0.214	0.275	0.241	0.224	0.78
Ethiopia	0.240	0.169	0.196	0.240	0.185	0.191	0.194	0.160	0.213	0.64
India	0.322	0.183	0.365	0.292	0.358	0.280	0.354	0.305	0.341	0.71
Malaysia	0.299	0.160	0.253	0.229	0.272	0.223	0.283	0.237	0.236	0.67

5.2 Flood Exposure

National flood exposure estimates calculated for each country using 35 different combinations of GFM and global population dataset are shown in *Figure* 2. No single GFM consistently predicted the most or least exposure across the five countries. The same is true for the global population datasets. In Colombia, Fathom predicted more than double the average exposure than any of the other GFMs. Here, Fathom's flood extent (152,304 km^2) was significantly larger relative to the other GFMs (the next largest extent is JRC at 87,961 km^2). In Malaysia, the model with the highest exposure was GLOFRIS. This was because it predicted far more exposure on the Malaysian coast than the other GFMs. This was a trend seen across the five countries, GLOFRIS predicted far more

coastal inundation than any other GFM. Flooding in level 6 coastal basins accounted for 21.5% of the total GLOFRIS flood extent, compared with 10.2% (CaMa-UT), 7.7% (Fathom), 7.2% (CIMA), and 6.8% (JRC). In each of the five countries, the average exposure calculated using Fathom was consistently above the 35-dataset exposure average, while exposure calculated using CaMa-UT and CIMA was consistently below the 35-dataset average.

The choice of global population dataset used also had a significant effect on exposure estimates. In Ethiopia, when LandScan and HRSL population maps were used, national flood exposure estimates were far lower across all the GFMs. In Colombia, flood exposure estimate disagreement in the Rio Negro basin to the south-east of the country was a result of the use of different population datasets rather than the use different GFMs. In this basin, average HRSL (47 thousand) and GHS-POP (39 thousand) exposures were far greater than Landscan (17 thousand), HYDE (9 thousand), WorldPop (8 thousand), GPW4 (4 thousand), and GRUMP (2 thousand) exposures. Much of this exposure disagreement in this basin came from the town of Mitú (see Figure in the Supplementary Material). Here, the GPW4 and GRUMP datasets did not even represent a town (populations below 100), WorldPop and HYDE picked up some population (below 4,000), only Landscan, GHS-POP, and HRSL represented population totals over 10,000 (2018 Mitú population estimate was 29,850 (DANE, 2019)). The difficulty in accurately representing rural towns and populations is one of the major contributing factors to exposure disagreement, especially if the population is exposed to a river as in Mitú. The population datasets agreed better in large urban areas. This is especially evident in *Figure 2* when examining the spread of the population exposure estimates for the JRC GFM in England. The majority (65%) of JRC's national exposure came from the Thames river in Greater London. Because the population datasets show greater agreement in dense urban areas, the differences in exposure estimates here are lower.
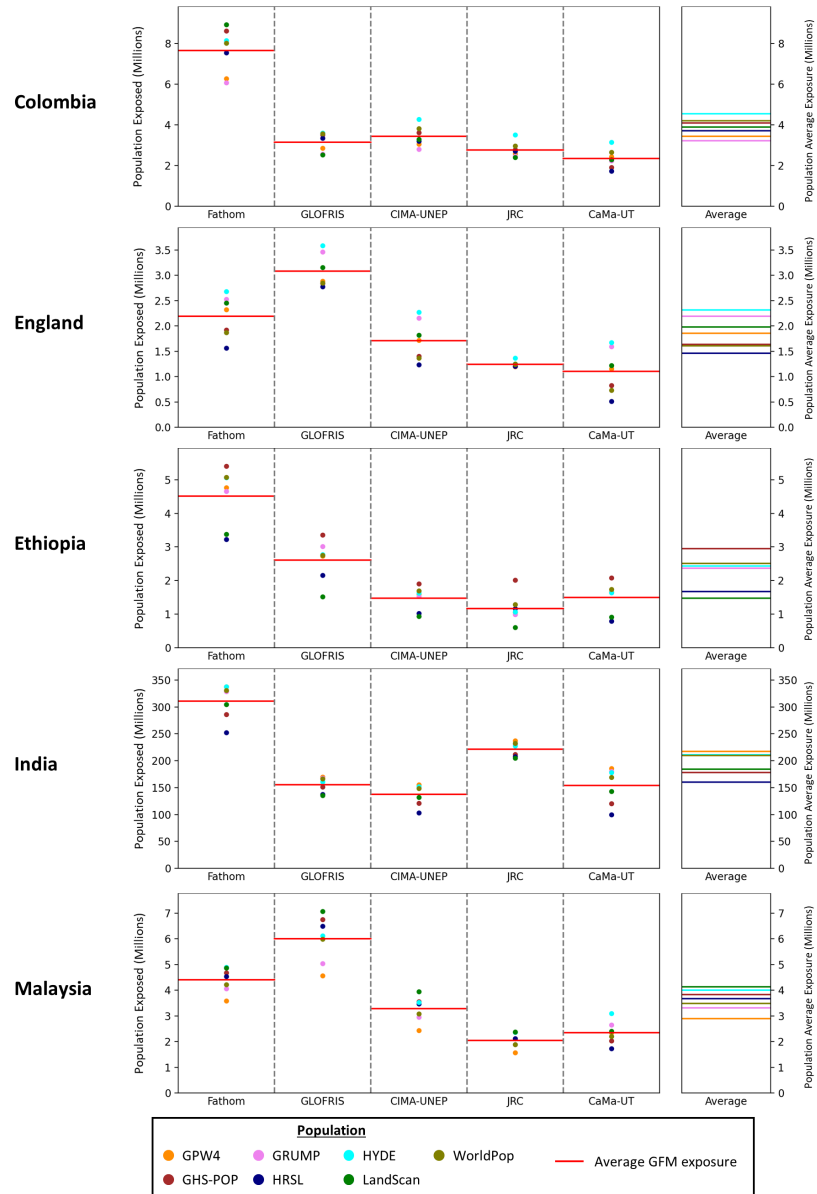
Figure 2. National flood exposure dot plots. 35 national flood exposure estimates calculated using five global flood models and seven global population datasets. Column on the right shows the average national flood exposure estimate calculated with each population dataset.

Across the five countries, the only population dataset whose average exposure showed a consistent trend above or below the 35-dataset average was HYDE, suggesting there are less cross-national trends in exposure estimates for global population data than there are for GFMs. The HYDE dataset maps population distribution at a resolution of nearly 9 km at the equator, which is between ten and three hundred times coarser than the other population datasets and between ten and one hundred times coarser than the GFMs. At such a coarse resolution, HYDE represents the interaction between the inundation and the exposure with significantly less precision, therefore, the resulting HYDE exposure estimates are influenced more by the modelled inundated area than the location of the population exposed. Conversely, HRSL exposure estimates were typically lower than the average (except for Malaysia). This is because the detailed representation of individual buildings in the HRSL dataset better captures the population's avoidance of obvious floodplains.
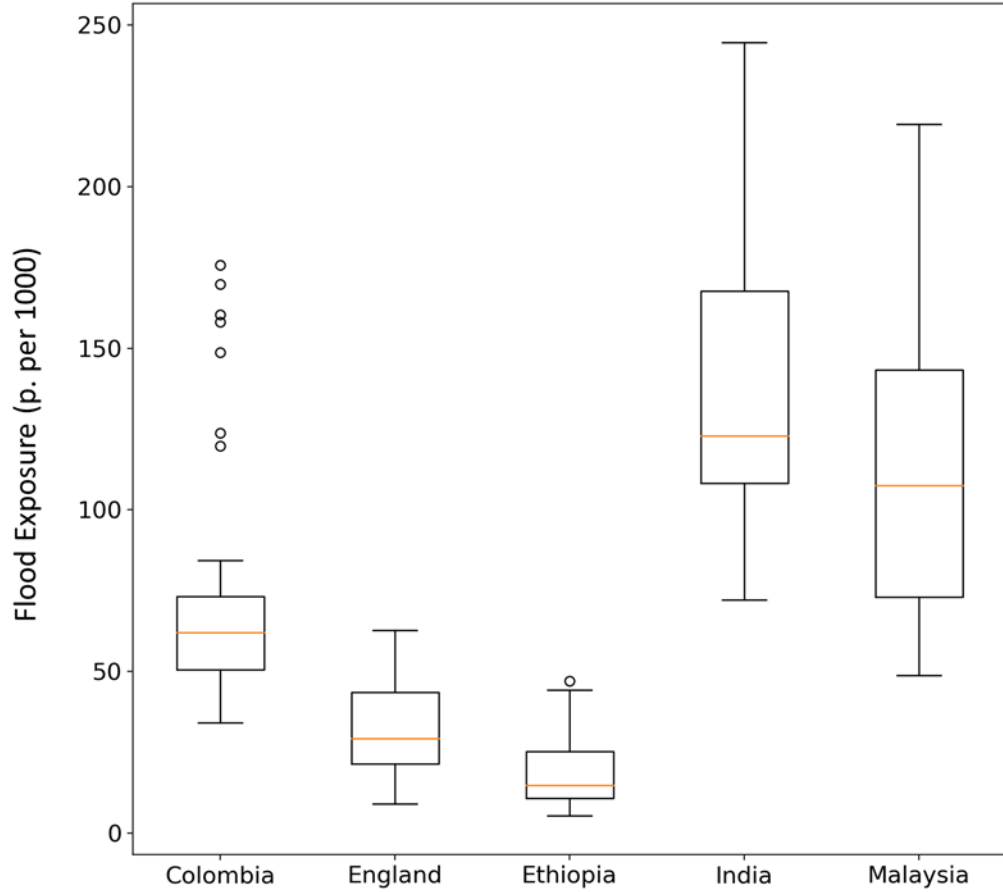
Figure 3. Box and whisker plots of normalized national flood exposure estimates for all five countries.

The spread of average GFM exposure is larger than the spread of average global population exposure in each of the five countries, suggesting that the choice of GFM used has a greater impact on exposure estimates than the choice of global population dataset used. To explore this further at the basin level, we compare the average coefficient of variation of flood exposure estimates when the choice of GFM is held constant to the average coefficient of variation when the choice of global population dataset is held constant. Across the five countries, we find that the choice of GFM had a greater influence on exposure estimates than the choice of population dataset in 90% of level 4 basins, 80% of level 5 basins, and 78% of level 6 basins. A figure identifying these basins is included in the Supplementary Material.

In *Figure 3*, exposure results are normalized and combined to produce box and

whisker plots for cross-country comparison. The distribution of national flood exposure estimates is comparatively smaller in England and Ethiopia than it is in Colombia, India, or Malaysia. The range of potential normalized national flood exposures calculated using global data in these three countries is substantial. In Colombia, normalized national exposure ranges between 34 and 175 people exposed per 1000; in India, it ranges between 72 and 244 people exposed per 1000; and in Malaysia, it ranges between 50 and 219 people exposed per 1000.

We also calculate population exposure to 20 years of historical flood events from the GFD. These exposure results are listed in *Table 4* along with exposure to the maximum combined GFM extent and exposure where the two datasets overlapped. The population dataset used to calculate exposure has an equally significant impact on observed flood exposure estimates as it does on modelled flood exposure estimates. For example in India, observed flood exposure calculated using HRSL (50 people per 1000) is 43% smaller than observed flood exposure calculated GPW4 (81.1 people per 1000). This is significant as often these datasets are used in immediate disaster response to estimate those exposed to flood events.

Table 4. Maximum combined Global Flood Model (Max GFM) and observed Global Flood Database (GFD) flood exposure comparison (exposed people per 1000)

Country	Flood Data	GPW4	GHS-POP	GRUMP	HRSL	HYDE	LandScan	WorldPop
Colombia	Max GFM	154.4	229	150.6	202	199.8	216.7	206.6
	GFD	11.4	12.1	11.3	9.9	13.5	16.7	13.6
	Overlap	9.5	6.2	9.5	5.3	10.7	7.8	9.9
England	Max GFM	92.1	84.7	104.7	77.1	108.3	99	83.3
	GFD	200.7	211.8	145.1	218.2	150.9	196.9	218.1
	Overlap	21	20.2	19.8	19.5	20.8	21.9	20.7
Ethiopia	Max GFM	63.5	71.3	65.2	44.9	65.4	42.7	64.7
	GFD	1.1	1.4	1.7	0.4	1.3	0.4	1.3
	Overlap	0.6	1.1	0.7	0.2	0.7	0.2	0.8
India	Max GFM	351.1	330.2	346.7	304.1	348.8	332.8	354.3
	GFD	88.1	54.4	82.3	50	81.5	65	80.7
	Overlap	76.4	42.7	71.1	39.5	69.3	51.8	68
Malaysia	Max GFM	252.6	347.5	278.6	337.9	327.5	369.6	311.9
	GFD	10.8	7	11.9	6.8	12.1	9.2	9
	Overlap	8.1	3.5	9.8	3.3	9.7	6.3	5.6

5.3 Flood Damages

Direct economic damages for the five countries were calculated using five GFMs and three different vulnerability approaches. The total economic damages and the GDP normalized economic damages for each country are shown in *Figure 4.* Total flood damages were largest in India: ranging from 29.7 billion EUR

(39.4 billion USD) to 109 billion EUR (145 billion USD) depending on the GFM and vulnerability approach used. Damages were most acute in Malaysia, where normalized damages made up between 2.2% and 29% of national GDP. Flood damages were comparatively small in Ethiopia, never exceeding 0.5% of national GDP. Here, when the GlobCover vulnerability approach was used, agricultural damages accounted for the majority of total damages (between 83% - 100%). Only two of the five GFMs (Fathom and CaMa-UT) calculated any urban Glob-Cover damages in Ethiopia. This is because the rivers running through the two cities where urban damages were calculated (Addis Ababa and Dawa) are too small to be modelled by three of the five GFMs.
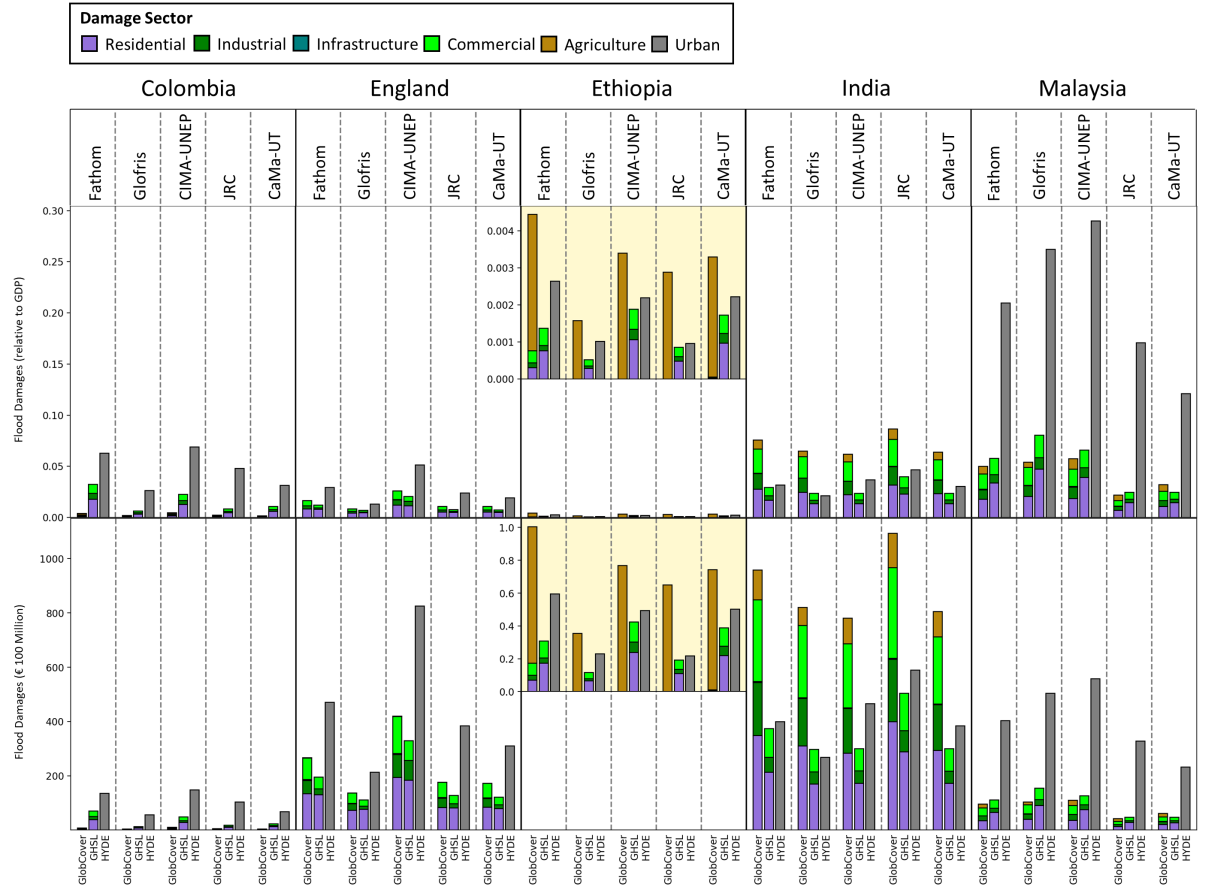
Figure 4. National flood damages calculated using five global flood models and three vulnerability approaches. (Top row) Normalized national flood damages (relative to national GDP). (Bottom row) Total national flood damages. Damages in 2010 Euros.

In each of the five countries, the choice of vulnerability approach used had a greater impact on direct damage estimates than the choice of GFM. In Colombia, the average total damages calculated using the GlobCover approach was 650 million EUR (862 million USD) compared to 3.5 billion EUR (4.6 billion USD) and 9.9 billion EUR (13.1 billion USD) when GHSL and HYDE approaches were used, respectively. No vulnerability approach consistently predicted the most or least damages. In Colombia, England, and Malaysia the HYDE method predicted the most damages, while in Ethiopia and India the GlobCover approach predicted the most damages. Differences in direct damages between the three approaches are a function of the land cover dataset used, and the assumptions made during the calculations. Apart from GlobCover, which also considers agriculture, damages are only calculated for urban areas. The three landcover datasets differ in their classification of urban areas. In Colombia, the total urban area defined by GlobCover was just 99 km^2, for GHSL it was 946 km^2, and for HYDE it was 2436 km^2. The differences in damages calculated in Colombia reflect these differences in urban area. This trend was similar in Malaysia, where urban areas were 1178 km^2, 1929 km^2, and 4929 km^2 for GlobCover, GHSL, and HYDE respectively. The three approaches make different assumptions about the categorization of damages. Inclusion of agricultural damages is significant in Ethiopia, but not in the other four countries. Infrastructure damages, which are only considered in the GlobCover approach, make up less than 2% of total damages in each of the five countries.

6 Discussion

6.1 Global data used nationally

We identify 16 different global flood risk datasets and methods that have been used in previous studies of global flood risk and use them to calculate national flood risk in five countries: Colombia, England, Ethiopia, India, and Malaysia. These datasets, which have been instrumental in improving our understanding of global flood risk over the past two decades, are becoming increasingly relevant at the national scale. However, as Ward et al. (2015) postulated about GFMs, "there is often a mismatch between their actual ability and the envisaged use by practitioners". We have shown that there is also mismatch between the different global datasets, which is reflected in what they tell us about national flood risk.

Disagreement between the GFMs is substantial, and this is reflected in their MAI scores. The scores, which range from 0.24-0.363, are in line with the scores of the intercomparison of the first generation of GFMs in Africa (Trigg et al., 2016). As the models develop, you would expect convergence in their modelled output. However, these models are not being developed at the same rate. Only three of the five GFMs tested in this study (Fathom, CaMa-UT, GLOFRIS) have updated their model outputs since the first Trigg et al. (2016) intercomparison. Fundamental differences between the models remain; most notably the thresholds set on the size of river modelled (Bernhofen et al., 2021). These thresholds impact estimates of flood risk at the national scale, as seen with the large Fathom risk estimates relative to the other models (especially in

Colombia and Ethiopia); and risk estimates at the basin and city scale, such as in the capital of Ethiopia, Addis Ababa, where only two of the five GFMs estimated any flood risk. Beyond differences in modelled domain, the models differ in their very structure. Although there are limits to the conclusions that can be drawn by a comparison of raw modelled output alone, results suggests differing levels of hydrodynamic representation and coastal boundary conditions contribute to disagreement in low-lying and coastal areas. This is evident across the five countries, but especially in England and Malaysia., the two countries with higher coast to area ratios. In these countries, GLOFRIS (a volume spreading model) predicts far higher coastal exposure, and subsequent national exposure, relative to the other (more hydrodynamic) models. The final resolution of the modelled flood extent should also be considered. The detail lost when using a 30 m or 90 m resolution flood map compared with a 1 km resolution flood map is not insignificant.

Equally important to globally modelled flood data is global observational flood data. Although the limits to this data have been shown in England, Ethiopia, and Malaysia. The incorrect classification of flooding from satellite imagery due to cloud or terrain shadows, as is apparent in England, can lead to significant over prediction of flooding and lead to potentially misclassified exposure (Revilla-Romero et al., 2015). In Ethiopia and Malaysia, the limited 20-year timeframe of the satellite observed data is evident, as the area of the country which is flooded is a small fraction of the 100-year return period GFM flooded area. Rather than used in isolation, global flood observations and GFM data should be used to complement each other (Hawker et al., 2020).

Population disagreement was almost as significant as GFM disagreement. This was most notable in rural areas, such as in south-east Colombia, where the town of Mitú was captured by only some of the population datasets. Global population data were classified in Leyk et al. (2019) by the complexity of modelled population distribution. Unmodelled population datasets, such as GPW4, evenly distribute population data over census enumerated areas. This means the detail at which population is represented is entirely dependent on the size of the enumerated areas; something which is highly variable across countries. In Colombia, where the size of the average census enumerated area is 1021 km^2, GPW4 calculated exposure is a lot less accurate than in England, where the size of the average census enumerated area is 0.76 km^2 (CIESIN, 2018). Indeed, it's surprising that GPW4 is still so widely used in studies of flood exposure, as it does not capture the population distribution at any detail finer than the census unit. The discrepancy in detail between national census data is something that needs to be considered for all population datasets that use GPW data as input (GHS-POP, GRUMP, HRSL, WorldPop), although the impact this has on final population estimates is smaller due to the additional population distribution modelling carried out by these datasets. The resolution of the population data is equally important to consider. The most resolved of the population datasets, HRSL, identifies individual dwellings at 30 m resolution. Highly resolved population data was shown in the studies of Smith et al. (2019) and Bernhofen et al.

(2021) to be of significant importance in accurately representing the avoidance of flood prone areas. Indeed, the low HRSL flood exposure estimates in four of the five countries examined in this study would support this finding. There are obvious limits to the conclusions that can be drawn with coarse resolution population data. Those datasets with a resolution of 1 km (GPW4, GRUMP, LandScan) will struggle to accurately model exposure on anything but the largest rivers. Even GHS-POP, which has a resolution of 250 m, was shown in Bernhofen et al. (2021) to be too coarse to accurately represent exposure on some smaller rivers. Certain population data, such as GRUMP and HYDE, are not relevant at the national scale. GRUMP, which has not been updated since 2000, is obsolete for flood risk analysis under current conditions. The HYDE data, at a resolution of roughly 9 km, is far too coarse to draw any meaningful conclusions at the national level. It was the only population dataset that consistently overpredicted exposure across the five countries examined. Population data should be chosen with the intended use in mind. Previous studies have highlighted the benefits of HRSL (Smith et al., 2019, Bernhofen et al., 2021), however, HRSL population estimates are limited to 2018. If consistent population estimates across time are required, datasets such as GHS-POP or WorldPop would be better suited. Similarly, if you want to calculate exposed day-time population rather than night-time population, Landscan is the only dataset you can use.

The range of low national VAI scores (0.132-0.217), which consider both extent and depth disagreement between the models, would suggest that the choice of GFM has a large effect on calculated national damages. What we found, was that the choice of vulnerability approach has a far greater effect on national damages than the choice of GFM. This was largely due to how the three different land cover maps used in the vulnerability calculations identified urban areas. Across the five countries, the size of urban area defined by each dataset was reflected in the national damage estimates. Equally important, but less reflected in the national flood damage estimates, was how the GlobCover and GHSL approaches split urban sector damages. Each approach applied constant global ratios of urban sector split, which were based on studies of either global or European cities (Dottori et al., 2018, Ward et al., 2020b). Sector level damages were directly impacted by these constant global ratios, meaning GHSL residential damages always made up a larger proportion of urban damages than GlobCover residential damages. The lack of a ceteris paribus comparison between vulnerability approaches limits the definite conclusions that can be drawn about the impact different aspects of the vulnerability calculation had on disagreement. Previous work by de Moel and Aerts (2011) found that the valuation of assets and the choice of damage curve had the greatest impact on damage uncertainty in the Dutch basin they were investigating. Similarly, when examining loss data in the US from the National Flood Insurance Program Wing et al. (2020) found that claims data does not fit the monotonic shape of traditional damage curves. It's well established that the vulnerability component of any flood risk assessment carries the most uncertainty at any scale. The assumptions and uncertainties associated with the three global vulnerability approaches tested in

this study do not translate well into the national context.

6.2 Uncertainty and decision making

Exploring the hazard, vulnerability and exposure components of flood risk using different models and datasets provides a useful basis for discussing uncertainty across all three components. Often quantifiable uncertainties are understood as risks, while unquantifiable uncertainties are understood as uncertainties. Some of these uncertainties are amenable to quantitative or qualitative evaluation, while some cannot be evaluated (Riesch, 2013). Key sources of modelling related uncertainty include; context and framing, input, model structure, parameter, and model technical uncertainty (Refsgaard et al., 2007). GFMs are not always developed for answering questions associated with context and framing, such as social, environmental, economic, technological, and infrastructural characteristics at the local scale. The extent to which these characteristics (often not accounted for) affect uncertainties differs from location to location and involves complex interactions. These characteristics may not always be captured in the calibration and validation process and does not always include all streamflow observation stations (Hirpa et al., 2021, Wing et al., 2021). This means that model parameterization is not always sensitive to local characteristics. Input data across GFMs suggests that there are commonalities (e.g. the DEM), interdependences, and differences making it difficult to isolate the impact of different factors on uncertainty. Substantial model structure, parameterization, and technical differences also mean that without a significantly complex sensitivity analysis it would be difficult to ascertain how and to what extent they individually or collectively affect uncertainty (Hoch and Trigg, 2019). As a consequence, while we use multiple models and datasets to illustrate uncertainties, the contribution of different sources of uncertainty is difficult to ascertain quantitatively or qualitatively.

With cascading uncertainty as GFM information is combined with exposure and vulnerability information from different datasets, there is an expansion of the uncertainty space. Flood risk assessments, based on the three components, would involve a further increase in uncertainty. Furthermore, the flood risk information may not always account for smaller scale flood prevention interventions or be relevant at hyperlocal scales where other socio-economic factors may affect flood risk. Further scrutiny may also reveal that there are important differences between extreme flood magnitudes (not explored in this study), as demonstrated in Africa (Trigg et al., 2016) and the conterminous United States (Devitt et al., 2021). There may also be other models, datasets, and even factors affecting risk that need to be accounted for to better understand risks. This suggests that although this study brings together multiple variants of the contributors to flood risk assessment, the uncertainty space is unclear and the contribution of different factors to exposure, damage and risk is not well characterized. This makes it challenging to interpret results in a way that can aid decision making at local scales. For instance, we discuss disagreement in typically flood prone areas like low-lying deltas and low relief coastal areas, and higher agreement

in larger river basins. This could affect the salience and credibility of the information for local to national level decision makers, some of whom may have primary knowledge and experience of dealing with flooding in such areas. Such information may be relevant to decision makers who are interested in hotspots and may focus on areas with greater agreement, or on areas where populations also face other hazards. An alternative way could be for decision makers to think of these different combinations (exposure, damage and risk) as scenarios that are plausible, but do not necessarily capture the full range of possibilities. Decision makers, who are often used to dealing with uncertainty, may find that a structured decision making under uncertainty approach (Bhave et al., 2016) may help assess the value of the information and make more informed flood management decisions.

6.3 National capacity to use global data

The inconsistencies and variation between these global datasets may call into question their 'usefulness' for evaluating flood risk, especially for some countries who experience limited institutional capacity and policy in FRM. The corroboration of global data with data collected locally may potentially ensure accuracy and consistency. However, the quality and availability of data in countries in the Global South is frequently very poor. For example, spatio-temporal time series are often not complete and bureaucratic, administrative barriers or political motivation can prevent access to data. These global datasets can hold exceptional value in areas that are data poor; for example, planetary level datasets have been used to detect long-term meteorological changes in Pakistan, India and Inner Mongolia (Lindersson et al., 2020).

Evaluations at the national scale may have limited impact on the most vulnerable of which usually inhabit agriculturally dependent rural areas, especially if population datasets are not resolved enough for these areas, or due to narrow or misaligned interpretations of vulnerability. For example, calculation of economic damage reflects inequality; hence it becomes important in relation to how something like agricultural damages are accounted for, given the centrality of agriculture in the livelihoods of many. whilst not economically catastrophic in GDP terms, this is potentially devastating on a local, livelihoods scale.

Effective FRM and the ability to use these global flood risk datasets requires policy and institutions that recognize the interconnected and interdependent systems that are inevitable, not only with technical interventions and infrastructure but also the socio-political networks that provide expertise and coordination (Jonkman and Dawson, 2012). However, the resources and agency to achieve this is frequently lacking, for example, some countries do not have specific FRM policies and with other disaster management areas taking priority, such as drought in Ethiopia and earthquakes in Colombia resulting in lack of agency regarding FRM.

7 Conclusions

As global flood risk data develops and becomes increasingly relevant at national

scales there is an urgent need to evaluate its credibility in a national flood risk context. By carrying out national flood risk assessments using global data in five different countries we explore the commonality and variability of global data used nationally. Global datasets vary significantly at the national level, and this is reflected in the national flood risk estimates. We find that the choice of GFM has a larger effect on exposure estimates than the choice of population dataset, while the choice of vulnerability approach has the greatest influence on national flood damage estimates. The detail of the datasets becomes increasingly important at the national scale. GFMs that do not model the flooding of small rivers are leaving a substantial amount of national flood risk unaccounted for. Similarly, coarse resolution global data limits the detail at which risk can be evaluated and diminishes the usefulness of certain datasets at this scale. Global approaches to calculating vulnerability are limited both by the uncertainty of global land cover datasets and the assumptions made to calculate damages at the global scale.

Further to these challenges and inconsistencies but just as significant is whether countries have the capacity to access and use these datasets. These datasets can only be effective if a country has a functioning, institutional framework with capability to support their use and implementation. This can include informed and proactive policies which both monitor and plan for future flood risk. Additionally, strong institutions that effectively implement these policies, which encourage expertise and assist the consultation and coordination between a diverse range of key stakeholders (Jonkman and Dawson, 2012). Technical and financial capital is significant in introducing and maintaining the infrastructure needed to monitor and assess flood-risk; as is the availability of good quality, compatible data to complement and use alongside these global datasets. Variation in the methods of conceptualizing population and vulnerability could be particularly problematic for compatibility.

8 Recommendations and future work

Global flood risk datasets were evaluated in this study by quantifying the uncertainty when used interchangeably for flood risk assessments at the national scale. Further work should incorporate locally sourced data and locally calibrated models to test the global datasets. Only then could one definitively conclude which data is 'best' for a given locality or use. These datasets could have considerable potential for assisting and furthering FRM in countries who have limited capacity to access local data, however further investigation is needed to reveal the extent to which countries find these datasets useful and have the capacity to use these datasets. Further work should examine in greater detail the institutional capability of national and local FRM to access and apply such datasets. The variation between these datasets also requires technical understanding of the nature of limitations of the data. Further, the application of such datasets as evidence for decision making entails choices over the allocation of resources. Future work should seek to examine the types of policy and resource allocations that result from the application of such datasets to FRM.

Data Availability

All the data used in this study is openly available for research purposes. CaMa-UT model outputs can be obtained from the developer at http://hydro.iis.u-tokyo.ac.jp/~yamadai/. Aggregated 1 km CIMA-UNEP flood maps can be downloaded from https://preview.grid.unep.ch, the native 3 arcsecond maps used in this study can be obtained directly from the developer. Fathom flood maps can be obtained from the developer at https://www.fathom.global/. GLOFRIS flood maps can be downloaded from the Aqueduct floods platform https://www.wri.org/applications/aqueduct/floods/. JRC flood maps can be downloaded from https://data.jrc.ec.europa.eu/collection/id-0054. The Global Flood Database maps can be downloaded from https://global-flood-database.cloudtostreet.ai/. The GPW4 population map can be downloaded from https://doi.org/10.7927/H4PN93PB. The GSH-POP population map can be downloaded from https://doi.org/10.2905/42E8BE89-54FF-464E-BE7B-BF9E64DA5218. The GRUMP population map can be downloaded from https://doi.org/10.7927/H4VT1Q1H. HRSL population maps can be downloaded from https://data.humdata.org/organization/facebook by searching 'population density'. The HYDE population map can be downloaded from https://dataportaal.pbl.nl/downloads/HYDE/. The LandScan population map can be downloaded from https://landscan.ornl.gov/landscan-datasets. World-Pop population maps can be downloaded from https://www.worldpop.org/geodata/listing?id=69. The GlobCover landcover map can be downloaded from http://due.esrin.esa.int/page_globcover.php. The GHSL built up area map can be downloaded from https://ghsl.jrc.ec.europa.eu/download.php?ds=bu. The HYDE fractional urban landcover map can be downloaded from https://dataportaal.pbl.nl/downloads/HYDE/.

References

AERTS, J. P. M., UHLEMANN-ELMER, S., EILANDER, D. & WARD, P. J. 2020. Comparison of estimates of global flood models for flood hazard and exposed gross domestic product: a China case study. *Nat. Hazards Earth Syst. Sci.,* 20**,** 3245-3260.AL JAZEERA. 2021. *Six dead, nearly 50,000 evacuated in Malaysia floods* [Online]. aljazeera.com: Al Jazeera. Available: https://www.aljazeera.com/news/2021/1/9/six-dead-nearly-50000-evacuated-in-malaysia-floods [Accessed 20 October 2021].ALEXANDER, M., PRIEST,

S. & MEES, H. 2016a. A framework for evaluating flood risk governance. *Environmental Science & Policy,* 64**,** 38-47.ALEXANDER, M., PRIEST, S. J., MICOU, P., TAPSELL, S. M., GREEN, C. H., PARKER, D. J. & HOMEWOOD, S. 2016b. Analysing and evaluating flood risk governance in England–enhancing societal resilience through comprehensive and aligned flood risk governance arrangements.ALFIERI, L., BUREK, P., DUTRA, E., KRZEMINSKI, B., MURARO, D., THIELEN, J. & PAPPENBERGER, F. 2013. GloFAS - global ensemble streamflow forecasting and flood early warning. *Hydrol. Earth Syst. Sci.,* 17**,** 1161-1175.ALFIERI, L., BISSELINK, B., DOTTORI, F., NAUMANN, G., DE ROO, A., SALAMON, P., WYSER, K. & FEYEN, L. 2017. Global projections of river flood risk in a warmer world. *Earths Future,* 5**,** 171-182.ALFIERI, L., DOTTORI, F., BETTS, R., SALAMON, P. & FEYEN, L. 2018. Multi-Model Projections of River Flood Risk in Europe under Global Warming. 6**,** 6. ALI, Q. S. W., PANDEY, S., CHAUDHURI, R. R., BEHERA, S. & JEYAKUMAR, L. 2021. Development of rainfall-infiltration measurement system and recharge strategies for urban flooding areas: a case study of Delhi, India. *Modeling Earth Systems and Environment,* 7**,** 2719-2731.ARNELL, N. W. & GOSLING, S. N. 2016. The impacts of climate change on river flood risk at the global scale. *Climatic Change,* 134**,** 387-401.BALK, D., POZZI, F., YETMAN, G., DEICHMANN, U. & NELSONC, A. 2005. The distribution of people and the dimension of place: Methodologies to improve the global estimation of urban extents. *International Society for Photogrammetry and Remote Sensing, Proceedings of the Urban Remote Sensing Conference.*BALK, D. L., DEICHMANN, U., YETMAN, G., POZZI, F., HAY, S. I. & NELSON, A. 2006. Determining Global Population Distribution: Methods, Applications and Data. *In:* HAY, S. I., GRAHAM, A. & ROGERS, D. J. (eds.) *Advances in Parasitology.* Academic Press.BALSAMO, G., BELJAARS, A., SCIPAL, K., VITERBO, P., VAN DEN HURK, B., HIRSCHI, M. & BETTS, A. K. 2009. A Revised Hydrology for the ECMWF Model: Verification from Field Site to Terrestrial Water Storage and Impact in the Integrated Forecast System %J Journal of Hydrometeorology. 10**,** 623-643.BALSAMO, G., ALBERGEL, C., BELJAARS, A., BOUSSETTA, S., BRUN, E., CLOKE, H., DEE, D., DUTRA, E., MUÑOZ-SABATER, J., PAPPENBERGER, F., DE ROSNAY, P., STOCKDALE, T. & VITART, F. 2015. ERA-Interim/Land: a global land surface reanalysis data set. *Hydrol. Earth Syst. Sci.,* 19**,** 389-407.BATES, P. D., HORRITT, M. S. & FEWTRELL, T. J. 2010. A simple inertial formulation of the shallow water equations for efficient two-dimensional flood inundation modelling. *Journal of Hydrology,* 387**,** 33-45.BATES, P. D., QUINN, N., SAMPSON, C., SMITH, A., WING, O., SOSA, J., SAVAGE, J., OLCESE, G., NEAL, J., SCHUMANN, G., GIUSTARINI, L., COXON, G., PORTER, J. R., AMODEO, M. F., CHU, Z., LEWIS-GRUSS, S., FREEMAN, N. B., HOUSER, T., DELGADO, M., HAMIDI, A., BOLLIGER, I., E. MCCUSKER, K., EMANUEL, K., FER- REIRA, C. M., KHALID, A., HAIGH, I. D., COUASNON, A., E. KOPP, R., HSIANG, S. & KRAJEWSKI, W. F. 2021. Combined Modeling of US Fluvial, Pluvial, and Coastal Flood Hazard Under Current and Future Climates. *Water*

Resources Research, 57**,** e2020WR028673. BERNHOFEN, M. V., TRIGG, M. A., SLEIGH, P. A., SAMPSON, C. C. & SMITH, A. M. 2021. Global flood exposure from different sized rivers. *Nat. Hazards Earth Syst. Sci.,* 21**,** 2829-2847.BERNHOFEN, M. V., WHYMAN, C., TRIGG, M. A., SLEIGH, P. A., SMITH, A. M., SAMPSON, C. C., YAMAZAKI, D., WARD, P. J., RUDARI, R., PAPPENBERGER, F., DOTTORI, F., SALAMON, P. & WINSEMIUS, H. C. 2018. A first collective validation of global fluvial flood models for major floods in Nigeria and Mozambique. *Environmental Research Letters,* 13.BESHIR, A. A. & SONG, J. 2021. Urbanization and its impact on flood hazard: the case of Addis Ababa, Ethiopia. *Natural Hazards: Journal of the International Society for the Prevention and Mitigation of Natural Hazards,* 109**,** 1167-1190.BHAVE, A. G., CONWAY, D., DESSAI, S. & STAINFORTH, D. A. 2016. Barriers and opportunities for robust decision making approaches to support climate change adaptation in the developing world. *Climate Risk Management,* 14**,** 1-10.BIRKMANN, J., DECH, S., HIRZINGER, G., KLEIN, R., KLÜPFEL, H., LEHMANN, F., MOTT, C., NAGEL, K., SCHLURMANN, T., SETIADI, N., SIEGERT, F. & STRUNZ, G. Measuring vulnerability to promote disaster-resilient societies: Conceptual frameworks and definitions. 2006.BONTEMPS, S., DEFOURNY, P., VAN BOGAERT, E., ARINO, O., KALOGIROU, V. & RAMOS PEREZ, J. 2011. GLOBCOVER 2009: Products Description and Validation Report. UCLouvain & ESA Team.BURBY, R. J. 2001. Flood insurance and floodplain management: the US experience. *Global Environmental Change Part B: Environmental Hazards,* 3**,** 111-122.CIESIN 2018. Gridded Population of the World, Version 4 (GPWv4): Administrative Unit Center Points with Population Estimates, Revision 11. Palisades, NY: NASA Socioeconomic Data and Applications Center (SEDAC).CORBANE, C., PESARESI, M., KEMPER, T., POLITIS, P., FLORCZYK, A. J., SYRRIS, V., MELCHIORRI, M., SABO, F. & SOILLE, P. 2019. Automated global delineation of human settlements from 40 years of Landsat satellite data archives. *Big Earth Data,* 3**,** 140-169.CWC, C. W. C. 2018. Comprehensive flood management in India.DANE 2019. Informacion Capital. Colombia: Departamento Administrativo Nacional de Estadistica (DANE).DAVIS, S. A. & SKAGGS, L. L. 1992. Catalog of residential depth-damage functions used by the army corps of engineers in flood damage estimation. ARMY ENGINEER INST FOR WATER RESOURCES ALEXANDRIA VA.DE MOEL, H. & AERTS, J. C. J. H. 2011. Effect of uncertainty in land use, damage models and inundation depth on flood damage estimates. *Natural Hazards,* 58**,** 407-425.DE MOEL, H., JONGMAN, B., KREIBICH, H., MERZ, B., PENNING-ROWSELL, E. & WARD, P. J. 2015. Flood risk assessments at different spatial scales. *Mitigation and Adaptation Strategies for Global Change,* 20**,** 865-890.DE, U., SINGH, G. & RASE, D. J. J. I. G. U. 2013. Urban flooding in recent decades in four mega cities of India. 17**,** 153-165.DEE, D. P., UPPALA, S. M., SIMMONS, A. J., BERRISFORD, P., POLI, P., KOBAYASHI, S., ANDRAE, U., BALMASEDA, M. A., BALSAMO, G., BAUER, P., BECHTOLD, P., BELJAARS, A. C. M., VAN DE BERG, L., BIDLOT, J., BORMANN, N., DELSOL, C., DRAGANI, R., FUENTES, M., GEER, A. J., HAIMBERGER,

L., HEALY, S. B., HERSBACH, H., HÓLM, E. V., ISAKSEN, L., KÅLLBERG, P., KÖHLER, M., MATRICARDI, M., MCNALLY, A. P., MONGE-SANZ, B. M., MORCRETTE, J.-J., PARK, B.-K., PEUBEY, C., DE ROSNAY, P., TAVOLATO, C., THÉPAUT, J.-N. & VITART, F. 2011. The ERA-Interim reanalysis: configuration and performance of the data assimilation system. 137**,** 553-597.DEVITT, L., NEAL, J., WAGENER, T. & COXON, G. 2021. Uncertainty in the extreme flood magnitude estimates of large-scale flood hazard models. *Environmental Research Letters,* 16**,** 064013.DILLEY, M., CHEN, R. S., DEICHMANN, U., L., L.-L. A. & ARNOLD, M. 2005. *Natural Disaster Hotsposts: A Global Risk Analysis,* Washington, DC, World Bank.DOTTORI, F. & TODINI, E. 2011. Developments of a flood inundation model based on the cellular automata approach: Testing different methods to improve model performance. *Physics and Chemistry of the Earth, Parts A/B/C,* 36**,** 266-280.DOTTORI, F., SALAMON, P., BIANCHI, A., ALFIERI, L., HIRPA, F. A. & FEYEN, L. 2016. Development and evaluation of a framework for global flood hazard mapping. *Advances in Water Resources,* 94**,** 87-102.DOTTORI, F., SZEWCZYK, W., CISCAR, J. C., ZHAO, F., ALFIERI, L., HIRABAYASHI, Y., BIANCHI, A., MONGELLI, I., FRIELER, K., BETTS, R. A. & FEYEN, L. 2018. Increased human and economic losses from river flooding with anthropogenic warming. *Nature Climate Change,* 8**,** 781-+.DOXSEY-WHITFIELD, E., MACMANUS, K., ADAMO, S. B., PISTOLESI, L., SQUIRES, J., BORKOVSKA, O. & BAPTISTA, S. R. 2015. Taking Advantage of the Improved Availability of Census Data: A First Look at the Gridded Population of the World, Version 4. *Papers in Applied Geography,* 1**,** 226-234.DRIESSEN, P. P. J., DIEPERINK, C., VAN LAERHOVEN, F., RUNHAAR, H. A. C. & VERMEULEN, W. J. V. 2012. Towards a Conceptual Framework for The Study of Shifts in Modes of Environmental Governance – Experiences From The Netherlands. *Environmental Policy and Governance,* 22**,** 143-160.DRIESSEN, P. P. J., HEGGER, D. L. T., KUNDZEWICZ, Z. W., VAN RIJSWICK, H. F. M. W., CRABBÉ, A., LARRUE, C., MATCZAK, P., PETTERSSON, M., PRIEST, S., SUYKENS, C., RAADGEVER, G. T. & WIERING, M. 2018. Governance Strategies for Improving Flood Resilience in the Face of Climate Change. 10**,** 1595.DRMFSS 2014. Disaster Risk Management Strategic Program and Investment Framework. Addis Ababa, Ethiopia: Ministry of Agriculture.DRYDEN, R., ANAND, M., LEHNER, B. & FLUET-CHOUINARD, E. 2021. Do we prioritize floodplains for development and farming? Mapping global dependence and exposure to inundation. *Global Environmental Change,* 71**,** 102370.ECONOMIDOU, M., ATANASIU, B., STANIASZEK, D., MAIO, J., NOLTE, I., RAPF, O., LAUSTSEN, J., RUYSSEVELT, P., STRONG, D. & ZINETTI, S. 2011. *Europe's buildings under the microscope. A country-by-country review of the energy performance of buildings.*EILANDER, D., COUASNON, A., IKEUCHI, H., MUIS, S., YAMAZAKI, D., WINSEMIUS, H. C. & WARD, P. J. 2020. The effect of surge on riverine flood hazard and impact in deltas globally. *Environmental Research Letters,* 15**,** 104007.ELVIDGE, C., BAUGH, K., HOBSON, V., KIHN, E., KROEHL, H., DAVIS, E. & COCERO, D. 1997. Satellite inventory of human

settlements using nocturnal radiation emissions: a contribution for the global toolchest. 3**,** 387-395.EMERTON, R., CLOKE, H., FICCHI, A., HAWKER, L., DE WIT, S., SPEIGHT, L., PRUDHOMME, C., RUNDELL, P., WEST, R., NEAL, J., CUNA, J., HARRIGAN, S., TITLEY, H., MAGNUSSON, L., PAPPENBERGER, F., KLINGAMAN, N. & STEPHENS, E. 2020. Emergency flood bulletins for Cyclones Idai and Kenneth: A critical evaluation of the use of global flood forecasts for international humanitarian preparedness and response. *International Journal of Disaster Risk Reduction,* 50**,** 101811.ENVIRONMENT AGENCY 2009. Flooding in England: A National Assessment of Flood Risk. Bristol: Environment Agency.FORREST, S., TRELL, E.-M. & WOLTJER, J. 2017. Flood Groups in England: Governance arrangements and contribution to flood resilience.FREIRE, S., KEMPER, T., PESARESI, M., FLORCZYK, A. & SYRRIS, V. Combining GHSL and GPW to improve global population mapping. 2015 IEEE International Geoscience and Remote Sensing Symposium (IGARSS), 26-31 July 2015 2015. 2541-2543.FREIRE, S., MACMANUS, K., PESARESI, M., DOXSEY-WHITFIELD, E. & MILLS, J. 2016. *Development of new open and free multi-temporal global population grids at 250 m resolution.*FREIRE, S., SCHIAVINA, M., FLORCZYK, A. J., MACMANUS, K., PESARESI, M., CORBANE, C., BORKOVSKA, O., MILLS, J., PISTOLESI, L., SQUIRES, J. & SLIUZAS, R. 2020. Enhanced data and methods for improving open and free global population grids: putting 'leaving no one behind' into practice. *International Journal of Digital Earth,* 13**,** 61-77.GARMESTANI, A. S. & BENSON, M. H. 2013. A Framework for Resilience-based Governance of Social-Ecological Systems. *Ecology and Society,* 18.GARVEY, A. & PAAVOLA, J. 2021. Community action on natural flood management and the governance of a catchment-based approach in the UK. n/a.GU, X., ZHANG, Q., LI, J., CHEN, D., SINGH, V. P., ZHANG, Y., LIU, J., SHEN, Z. & YU, H. 2020. Impacts of anthropogenic warming and uneven regional socio-economic development on global river flood risk. *Journal of Hydrology,* 590**,** 125262.GUNDERSON, L. H. & S, H. C. 2002. *Panarchy: understanding transformations in human and natural systems,* Washington DC, USA, Island Press.HAILE, A. T., HABIB, E. & RIENTJES, T. 2013a. Evaluation of the climate prediction center (CPC) morphing technique (CMORPH) rainfall product on hourly time scales over the source of the Blue Nile River. 27**,** 1829-1839.HAILE, A. T., KUSTERS, K. & WAGESHO, N. 2013b. Loss and damage from flooding in the Gambela region, Ethiopia. *International Journal of Global Warming,* 5**,** 483-497.HALL, J. W. 2014. Editorial: steps towards global flood risk modelling. *Journal of Flood Risk Management,* 7**,** 193-194.HALL, J. W., DAWSON, R. J., SAYERS, P. B., ROSU, C., CHATTERTON, J. B. & DEAKIN, R. 2003. A methodology for national-scale flood risk assessment. 156**,** 235-247.HALL, J. W., SAYERS, P. B. & DAWSON, R. J. 2005. National-scale Assessment of Current and Future Flood Risk in England and Wales. *Natural Hazards,* 36**,** 147-164.HAWKER, L., NEAL, J., TELLMAN, B., LIANG, J., SCHUMANN, G., DOYLE, C., SULLIVAN, J. A., SAVAGE, J. & TSHIMANGA, R. 2020. Comparing earth observation and inundation models to map flood hazards. *Environmental*

Research Letters, 15**,** 124032.HAZELEGER, W., WANG, X., SEVERIJNS, C., ȘTEFĂNESCU, S., BINTANJA, R., STERL, A., WYSER, K., SEMMLER, T., YANG, S., VAN DEN HURK, B., VAN NOIJE, T., VAN DER LINDEN, E. & VAN DER WIEL, K. 2012. EC-Earth V2.2: description and validation of a new seamless earth system prediction model. *Climate Dynamics,* 39**,** 2611-2629.HIRABAYASHI, Y., KANAE, S., EMORI, S., OKI, T. & KIMOTO, M. 2008. Global projections of changing risks of floods and droughts in a changing climate. Hydrological Sciences Journal.HIRABAYASHI, Y., MAHENDRAN, R., KOIRALA, S., KONOSHIMA, L., YAMAZAKI, D., WATANABE, S., KIM, H. & KANAE, S. 2013. Global flood risk under climate change. *Nature Climate Change,* 3**,** 816-821.HIRABAYASHI, Y., TANOUE, M., SASAKI, O., ZHOU, X. & YAMAZAKI, D. 2021. Global exposure to flooding from the new CMIP6 climate model projections. *Scientific Reports,* 11**,** 3740.HIRPA, F. A., LORINI, V., DADSON, S. J. & SALAMON, P. 2021. Calibration of Global Flood Models. *Global Drought and Flood.*HOCH, J. M. & TRIGG, M. A. 2019. Advancing global flood hazard simulations by improving comparability, benchmarking, and integration of global flood models. *Environmental Research Letters,* 14**,** 034001.HOYOS, N., ESCOBAR, J., RESTREPO, J. C., ARANGO, A. M. & ORTIZ, J. C. 2013. Impact of the 2010–2011 La Niña phenomenon in Colombia, South America: The human toll of an extreme weather event. *Applied Geography,* 39**,** 16-25.HUIZINGA, K., DE MOEL, H. & SZEWCZYK, W. 2017. Global flood depth-damage functions. Methodology and the database with guidelines. JRC Technical Reports.JONGMAN, B., WARD, P. J. & AERTS, J. 2012. Global exposure to river and coastal flooding: Long term trends and changes. *Global Environmental Change-Human and Policy Dimensions,* 22**,** 823-835.JONKMAN, S. N. & DAWSON, R. J. 2012. Issues and Challenges in Flood Risk Management—Editorial for the Special Issue on Flood Risk Management. 4**,** 785-792.KENDON, M., MCCARTHY, M., JEVREJEVA, S., MATTHEWS, A. & LEGG, T. 2019. State of the UK climate 2018. 39**,** 1-55.KETTNER, A. J., BRAKENRIDGE, G. R., SCHUMANN, G. J. P. & SHEN, X. 2021. Chapter 7 - DFO—Flood Observatory. *In:* SCHUMANN, G. J. P. (ed.) *Earth Observation for Flood Applications.* Elsevier.KLEIN GOLDEWIJK, K., BEUSEN, A. & JANSSEN, P. 2010. Long-term dynamic modeling of global population and built-up area in a spatially explicit way: HYDE 3.1. 20**,** 565-573.KLEIN GOLDEWIJK, K., BEUSEN, A., DOELMAN, J. & STEHFEST, E. 2017. Anthropogenic land use estimates for the Holocene – HYDE 3.2. *Earth Syst. Sci. Data,* 9**,** 927-953.KLIJN, F., BAAN, P., DE BRUIJN, K., KWADIJK, J. & VAN BUREN, R. 2007. Overstromingsrisico's in Nederland in een veranderend klimaat: Verwachtingen, schattingen en berekeningen voor het project Nederland Later.KOK, M. 2004. *Standaardmethode 2004: Schade en slachtoffers als gevolg van overstromingen*, Ministerie van Verkeer en Waterstaat, Rijkswaterstaat.LEHNER, B., VERDIN, K. & JARVIS, A. 2008. New Global Hydrography Derived From Spaceborne Elevation Data. *Eos, Transactions American Geophysical Union,* 89**,** 93-94.LEHNER, B. & GRILL, G. 2013. Global river hydrography and network routing: baseline data and new approaches to study the world's

large river systems. Hydrological Processes.LEYK, S., GAUGHAN, A. E., ADAMO, S. B., DE SHERBININ, A., BALK, D., FREIRE, S., ROSE, A., STEVENS, F. R., BLANKESPOOR, B., FRYE, C., COMENETZ, J., SORICHETTA, A., MACMANUS, K., PISTOLESI, L., LEVY, M., TATEM, A. J. & PESARESI, M. 2019. The spatial allocation of population: a review of large-scale gridded population data products and their fitness for use. *Earth Syst. Sci. Data,* 11**,** 1385-1409.LINDERSSON, S., BRANDIMARTE, L., MÅRD, J. & DI BALDASSARRE, G. 2020. A review of freely accessible global datasets for the study of floods, droughts and their interactions with human societies. *WIREs Water,* 7**,** e1424.LINDERSSON, S., BRANDIMARTE, L., MÅRD, J. & DI BALDASSARRE, G. 2021. Global riverine flood risk – how do hydrogeomorphic floodplain maps compare to flood hazard maps? *Nat. Hazards Earth Syst. Sci.,* 21**,** 2921-2948.LINKE, S., LEHNER, B., OUEL-LET DALLAIRE, C., ARIWI, J., GRILL, G., ANAND, M., BEAMES, P., BURCHARD-LEVINE, V., MAXWELL, S., MOIDU, H., TAN, F. & THIEME, M. 2019. Global hydro-environmental sub-basin and river reach characteristics at high spatial resolution. *Scientific Data,* 6**,** 283.LLOYD, C. T., CHAM-BERLAIN, H., KERR, D., YETMAN, G., PISTOLESI, L., STEVENS, F. R., GAUGHAN, A. E., NIEVES, J. J., HORNBY, G., MACMANUS, K., SINHA, P., BONDARENKO, M., SORICHETTA, A. & TATEM, A. J. 2019. Global spatio-temporally harmonised datasets for producing high-resolution gridded population distribution datasets. *Big Earth Data,* 3**,** 108-139.LOESCHNER, L., NORDBECK, R., SCHINDLEGGER, A. & SEHER, W. 2019. COMPENSAT-ING FLOOD RETENTION ON PRIVATE LAND IN AUSTRIA: TOWARDS POLYCENTRIC GOVERNANCE IN FLOOD RISK MANAGEMENT? 7**,** 32-45.MABAHWI, N. A., NAKAMURA, H. & BHATTACHARYA, Y. 2020. Flood Risk Management in Malaysia: The current hindrances for flood related agencies. *Asian Journal of Behavioural Studies,* 5**,** 11-24.MERZ, B., HALL, J., DISSE, M. & SCHUMANN, A. 2010. Fluvial flood risk management in a changing world. *Nat. Hazards Earth Syst. Sci.,* 10**,** 509-527.MESTER, B., WILLNER, S. N., FRIELER, K. & SCHEWE, J. 2021. Evaluation of river flood extent simulated with multiple global hydrological models and climate forcings. *Environmental Research Letters,* 16**,** 094010.MEYER, V., BECKER, N., MARKANTONIS, V., SCHWARZE, R., VAN DEN BERGH, J. C. J. M., BOUWER, L. M., BUBECK, P., CIAVOLA, P., GENOVESE, E., GREEN, C., HALLEGATTE, S., KREIBICH, H., LEQUEUX, Q., LOGAR, I., PAPYRAKIS, E., PFURTSCHELLER, C., POUSSIN, J., PRZYLUSKI, V., THIEKEN, A. H. & VIAVATTENE, C. 2013. Review article: Assessing the costs of natural hazards – state of the art and knowledge gaps. *Nat. Hazards Earth Syst. Sci.,* 13**,** 1351-1373.MORRISON, A., WESTBROOK, C. J. & NOBLE, B. F. 2018. A review of the flood risk management gov-ernance and resilience literature. *Journal of Flood Risk Management,* 11**,** 291-304.MUNICHRE. *Risks from floods, storm surges and flash floods* [Online]. Available: https://www.munichre.com/en/risks/natural-disasters-losses-are-trending-upwards/floods-and-flash-floods-underestimated-natural-hazards.html [Accessed May 5 2021].NEAL, J., SCHUMANN, G. & BATES, P. 2012. A

subgrid channel model for simulating river hydraulics and floodplain inundation over large and data sparse areas. *Water Resources Research,* 48**,** 16.NEAL, J., HAWKER, L., SAVAGE, J., DURAND, M., BATES, P. & SAMPSON, C. 2021. Estimating River Channel Bathymetry in Large Scale Flood Inundation Models. 57**,** e2020WR028301.PAPPENBERGER, F., BEVEN, K., FRODSHAM, K., ROMANOWICZ, R. & MATGEN, P. 2007. Grasping the unavoidable subjectivity in calibration of flood inundation models: A vulnerability weighted approach. *Journal of Hydrology,* 333**,** 275-287.PENNING-ROWSELL, E. C., PRIEST, S. J., PARKER, D. J., MORRIS, J., TUNSTALL, S. M. V., VIAVATTENE, C., CHATTERTON, J. & OWEN, D. 2013. *Flood and coastal erosion risk management: a manual for economic appraisal,* London, U.K., Routledge, Taylor & Francis.PESARESI, M., HUADONG, G., BLAES, X., EHRLICH, D., FERRI, S., GUEGUEN, L., HALKIA, M., KAUFFMANN, M., KEMPER, T., LU, L., MARIN-HERRERA, M. A., OUZOUNIS, G. K., SCAVAZZON, M., SOILLE, P., SYRRIS, V. & ZANCHETTA, L. 2013. A Global Human Settlement Layer From Optical HR/VHR RS Data: Concept and First Results. *IEEE Journal of Selected Topics in Applied Earth Observations and Remote Sensing,* 6**,** 2102-2131.PESARESI, M., EHRLICH, D., FLORCZYK, A. J., FREIRE, S., JULEA, A., KEMPER, T. & SYRRIS, V. The global human settlement layer from landsat imagery. 2016 IEEE International Geoscience and Remote Sensing Symposium (IGARSS), 10-15 July 2016 2016. 7276-7279.RAMIREZ-VILLEGAS, J., SALAZAR, M., JARVIS, A. & NAVARRO-RACINES, C. E. 2012. A way forward on adaptation to climate change in Colombian agriculture: perspectives towards 2050. *Climatic Change,* 115**,** 611-628.RAY, K., PANDEY, P., PANDEY, C., DIMRI, A. P. & KISHORE, K. 2019. On the Recent Floods in India. *Current science,* 117.REFSGAARD, J. C., VAN DER SLUIJS, J. P., HØJBERG, A. L. & VANROLLEGHEM, P. A. 2007. Uncertainty in the environmental modelling process – A framework and guidance. *Environmental Modelling & Software,* 22**,** 1543-1556.RENTSCHLER, J. & SALHAB, M. 2020. People in Harm's Way: Flood Exposure and Poverty in 189 Countries. *Policy Research Wokring Paper.* Washington, D.C.: World Bank.REVILLA-ROMERO, B., HIRPA, F. A., POZO, J. T.-D., SALAMON, P., BRAKENRIDGE, R., PAPPENBERGER, F. & DE GROEVE, T. 2015. On the Use of Global Flood Forecasts and Satellite-Derived Inundation Maps for Flood Monitoring in Data-Sparse Regions. 7**,** 15702-15728.RIESCH, H. 2013. Levels of Uncertainty. *In:* ROESER, S., HILLERBRAND, R., SANDIN, P. & PETERSON, M. (eds.) *Essentials of Risk Theory.* Dordrecht: Springer Netherlands.RUDARI, R., SILVESTRO, F., CAMPO, L., REBORA, N., BONI, G. & HEROLD, C. 2015. IMPROVEMENT OF THE GLOBAL FLOOD MODEL FOR THE GAR 2015.SAIFULSYAHIRA, J., EDRE, M., AF, A. F., JUNI, M. H. J. I. J. O. P. H. & SCIENCES, C. 2016. Governance of flood disaster management: Malaysian case study. 3**,** 17-30.SAMPSON, C. C., SMITH, A. M., BATES, P. B., NEAL, J. C., ALFIERI, L. & FREER, J. E. 2015. A high-resolution global flood hazard model. *Water Resources Research,* 51**,** 7358-7381.SCHELFAUT, K., PANNEMANS, B., VAN DER CRAATS, I., KRYWKOW, J., MYSIAK, J. & COOLS, J. 2011. Bringing

flood resilience into practice: the FREEMAN project. *Environmental Science & Policy,* 14**,** 825-833.SCHELLEKENS, J., DUTRA, E., MARTINEZ-DE LA TORRE, A., BALSAMO, G., VAN DIJK, A., WEILAND, F. S., MINVIELLE, M., CALVET, J. C., DECHARME, B., EISNER, S., FINK, G., FLORKE, M., PESSENTEINER, S., VAN BEEK, R., POLCHER, J., BECK, H., ORTH, R., CALTON, B., BURKE, S., DORIGO, W. & WEEDON, G. P. 2017. A global water resources ensemble of hydrological models: the eartH2Observe Tier-1 dataset. *Earth System Science Data,* 9**,** 389-413.SILVESTRO, F., GABEL-LANI, S., DELOGU, F., RUDARI, R. & BONI, G. 2013. Exploiting remote sensing land surface temperature in distributed hydrological modelling: the example of the Continuum model. *Hydrol. Earth Syst. Sci.,* 17**,** 39-62.SMITH, A., SAMPSON, C. & BATES, P. 2015. Regional flood frequency analysis at the global scale. *Water Resources Research,* 51**,** 539-553.SMITH, A., BATES, P. D., WING, O., SAMPSON, C., QUINN, N. & NEAL, J. 2019. New estimates of flood exposure in developing countries using high-resolution population data. *Nature Communications,* 10**,** 1814.STEVENS, F. R., GAUGHAN, A. E., LINARD, C. & TATEM, A. J. 2015. Disaggregating Census Data for Population Mapping Using Random Forests with Remotely-Sensed and Ancillary Data. *Plos One,* 10**,** 22.SUTANUDJAJA, E. H., VAN BEEK, R., WANDERS, N., WADA, Y., BOSMANS, J. H. C., DROST, N., VAN DER ENT, R. J., DE GRAAF, I. E. M., HOCH, J. M., DE JONG, K., KARSSENBERG, D., LÓPEZ LÓPEZ, P., PEßENTEINER, S., SCHMITZ, O., STRAATSMA, M. W., VANNAMETEE, E., WISSER, D. & BIERKENS, M. F. P. 2018. PCR-GLOBWB 2: a 5 arcmin global hydrological and water resources model. *Geosci. Model Dev.,* 11**,** 2429-2453.TANOUE, M., HIRABAYASHI, Y. & IKEUCHI, H. 2016. Global-scale river flood vulnerability in the last 50 years. *Scientific Reports,* 6**,** 36021.TELLMAN, B., SULLIVAN, J. A., KUHN, C., KETTNER, A. J., DOYLE, C. S., BRAKENRIDGE, G. R., ERICKSON, T. A. & SLAYBACK, D. A. 2021. Satellite imaging reveals increased proportion of population exposed to floods. *Nature,* 596**,** 80-86.TIECKE, T. G. L., XIAN-MING ZHANG, AMY GROS, ANDREAS LI, NAN YETMAN, GREGORY KILIC, TALIP MURRAY, SIOBHAN BLANKESPOOR, BRIAN PRYDZ, ESPEN B. DANG, HAI-ANH H. 2017. *Mapping the World Population One Building at a Time.*THOMSON, D. R., GAUGHAN, A. E., STEVENS, F. R., YETMAN, G., ELIAS, P. & CHEN, R. 2021. Evaluating the Accuracy of Gridded Population Estimates in Slums: A Case Study in Nigeria and Kenya. 5**,** 48.TIECKE, T. G. L., XIANMING ZHANG, AMY GROS, ANDREAS LI, NAN YETMAN, GREGORY KILIC, TALIP MURRAY, SIOBHAN BLANKESPOOR, BRIAN PRYDZ, ESPEN B. DANG, HAI-ANH H. 2017. *Mapping the World Population One Building at a Time.*TRENDS 2020. Leaving no one off the map: a guide for gridded population data for sustainable development. Thematic Research Network on Data and Statistics.TRIGG, M. A., BERNHOFEN, M. V., MARECHAL, D., ALFIERI, L., DOTTORI, F., HOCH, J. M., HORRITT, M. S., SAMPSON, C., SMITH, A., YAMAZAKI, D. & LI, H. Y. 2020. Global Flood Models. *American Geophysical Union Monograph: Global drought and flood.* Wiley.TRIGG, M. A., BIRCH, C. E.,

NEAL, J. C., BATES, P. D., SMITH, A., SAMPSON, C. C., YAMAZAKI, D., HIRABAYASHI, Y., PAPPENBERGER, F., DUTRA, E., WARD, P. J., WINSEMIUS, H. C., SALAMON, P., DOTTORI, F., RUDARI, R., KAPPES, M. S., SIMPSON, A. L., HADZILACOS, G. & FEWTRELL, T. J. 2016. The credibility challenge for global fluvial flood risk analysis. *Environmental Research Letters,* 11**,** 10.UNDRR 2015. Global Assessment Report 2015, Making Development Sustainable: The Future of Disaster Risk Management. Geneva: UN Office for Disaster Risk Reduction UNDRR 2020. *Human Cost of Disasters: An overview of the last 20 years 2000-2019*, United Nations.UNISDR 2004. Living with risk: a global review of disaster reduction initiatives. United Nations for Disaster Risk Reduction (UNISDR).UNISDR 2015. Sendai Framework for Disaster Risk Reduction 2015-2030. United Nations - Headquarters (UN).VAN BEEK, L. P. H., WADA, Y. & BIERKENS, M. F. P. 2011. Global monthly water stress: 1. Water balance and water availability. 47.VAN WESENBEECK, B. K., MULDER, J. P. M., MARCHAND, M., REED, D. J., DE VRIES, M. B., DE VRIEND, H. J. & HERMAN, P. M. J. 2014. Damming deltas: A practice of the past? Towards nature-based flood defenses. *Estuarine, Coastal and Shelf Science,* 140**,** 1-6.VAN WESTEN, C. J. 2014. Vulnerability. *Caribbean Handbook on Risk Management: Methodology Book.* Carribean Disaster Emergency Managment Agency.VENOT, J.-P., BOWERS, S., BROCKINGTON, D., KOMAKECH, H., RYAN, C. M., VELDWISCH, G. J. & WOODHOUSE, P. J. W. A. 2021. Below the Radar: Data, Narratives and the Politics of Irrigation in Sub-Saharan Africa. 14**,** 546-572.VINNARASI, R. & DHANYA, C. T. 2016. Changing characteristics of extreme wet and dry spells of Indian monsoon rainfall. 121**,** 2146-2160.WARD, P. J., JONGMAN, B., WEILAND, F. S., BOUWMAN, A., VAN BEEK, R., BIERKENS, M. F. P., LIGTVOET, W. & WINSEMIUS, H. C. 2013. Assessing flood risk at the global scale: model setup, results, and sensitivity. *Environmental Research Letters,* 8**,** 10.WARD, P. J., JONGMAN, B., SALAMON, P., SIMPSON, A., BATES, P., DE GROEVE, T., MUIS, S., DE PEREZ, E. C., RUDARI, R., TRIGG, M. A. & WINSEMIUS, H. C. 2015. Usefulness and limitations of global flood risk models. *Nature Climate Change,* 5**,** 712-715.WARD, P. J., JONGMAN, B., AERTS, J., BATES, P. D., BOTZEN, W. J. W., LOAIZA, A. D., HALLEGATTE, S., KIND, J. M., KWADIJK, J., SCUSSOLINI, P. & WINSEMIUS, H. C. 2017. A global framework for future costs and benefits of river-flood protection in urban areas. *Nature Climate Change,* 7**,** 642-+.WARD, P. J., BLAUHUT, V., BLOEMENDAAL, N., DANIELL, J. E., DE RUITER, M. C., DUNCAN, M. J., EMBERSON, R., JENKINS, S. F., KIRSCHBAUM, D., KUNZ, M., MOHR, S., MUIS, S., RIDDELL, G. A., SCHÄFER, A., STANLEY, T., VELDKAMP, T. I. E. & WINSEMIUS, H. C. 2020a. Review article: Natural hazard risk assessments at the global scale. *Nat. Hazards Earth Syst. Sci.,* 20**,** 1069-1096.WARD, P. J., WINSEMIUS, H. C., KUZMA, S., BIERKENS, M. F. P., BOUWMAN, A., DE MOEL, H., DÍAZ LOAIZA, A., EILANDER, D., ENGLHARDT, J., ERKENS, G., TAFETE GEBTEMEDHIN, E., ICELAND, C., KOOI, H., LIGTVOET, W., MUIS, S., SCUSSOLINI, P., SUTANUDJAJA, E. H., VAN BEEK, R., VAN BEMMEL,

B., VAN HUIJSTEE, J., VAN RIJN, F., VAN WESENBEECK, B., VATVANI, D., VERLAAN, M., TIGGELOVEN, T. & LUO, T. 2020b. Aqueduct Floods Methodology. Wasington D.C.: World Resources Institute.WEEDON, G. P., GOMES, S., VITERBO, P., SHUTTLEWORTH, W. J., BLYTH, E., ÖSTERLE, H., ADAM, J. C., BELLOUIN, N., BOUCHER, O. & BEST, M. 2011. Creation of the WATCH Forcing Data and Its Use to Assess Global and Regional Reference Crop Evaporation over Land during the Twentieth Century. *Journal of Hydrometeorology,* 12**,** 823-848.WEEDON, G. P., BALSAMO, G., BELLOUIN, N., GOMES, S., BEST, M. J. & VITERBO, P. 2014. The WFDEI meteorological forcing data set: WATCH Forcing Data methodology applied to ERA-Interim reanalysis data. 50**,** 7505-7514.WILLNER, S. N., OTTO, C. & LEVERMANN, A. 2018. Global economic response to river floods. *Nature Climate Change,* 8**,** 594-598.WING, O. E. J., BATES, P. D., SAMPSON, C. C., SMITH, A. M., JOHNSON, K. A. & ERICKSON, T. A. 2017. Validation of a 30 m resolution flood hazard model of the conterminous United States. *Water Resources Research,* 53**,** 7968-7986.WING, O. E. J., BATES, P. D., SMITH, A. M., SAMPSON, C. C., JOHNSON, K. A., FARGIONE, J. & MOREFIELD, P. 2018. Estimates of present and future flood risk in the conterminous United States. *Environmental Research Letters,* 13**,** 7.WING, O. E. J., BATES, P. D., NEAL, J. C., SAMPSON, C. C., SMITH, A. M., QUINN, N., SHUSTIKOVA, I., DOMENEGHETTI, A., GILLES, D. W., GOSKA, R. & KRAJEWSKI, W. F. 2019. A New Automated Method for Improved Flood Defense Representation in Large-Scale Hydraulic Models. *Water Resources Research,* 55**,** 11007-11034.WING, O. E. J., PINTER, N., BATES, P. D. & KOUSKY, C. 2020. New insights into US flood vulnerability revealed from flood insurance big data. *Nature Communications,* 11**,** 1444.WING, O. E. J., SMITH, A. M., MARSTON, M. L., PORTER, J. R., AMODEO, M. F., SAMPSON, C. C. & BATES, P. D. 2021. Simulating historical flood events at the continental scale: observational validation of a large-scale hydrodynamic model. *Nat. Hazards Earth Syst. Sci.,* 21**,** 559-575.WINSEMIUS, H. C., VAN BEEK, L. P. H., JONGMAN, B., WARD, P. J. & BOUWMAN, A. 2013. A framework for global river flood risk assessments. *Hydrology and Earth System Sciences,* 17**,** 1871-1892.WINSEMIUS, H. C., AERTS, J., VAN BEEK, L. P. H., BIERKENS, M. F. P., BOUWMAN, A., JONGMAN, B., KWADIJK, J. C. J., LIGTVOET, W., LUCAS, P. L., VAN VUUREN, D. P. & WARD, P. J. 2016. Global drivers of future river flood risk. *Nature Climate Change,* 6**,** 381-385.WISSMAN-WEBER, N. K. & LEVY, D. L. 2018. Climate adaptation in the Anthropocene: Constructing and contesting urban risk regimes. *Organization,* 25**,** 491-516.YAMAZAKI, D., KANAE, S., KIM, H. & OKI, T. 2011. A physically based description of floodplain inundation dynamics in a global river routing model. *Water Resources Research,* 47**,** 21.YAMAZAKI, D., DE ALMEIDA, G. A. M. & BATES, P. D. 2013. Improving computational efficiency in global river models by implementing the local inertial flow equation and a vector-based river network map. Water Resources Research.YAMAZAKI, D., SATO, T., KANAE, S., HIRABAYASHI, Y. & BATES, P. D. 2014. Regional flood dynamics in a bifurcating mega delta simulated in a global river model.

Geophysical Research Letters, 41**,** 3127-3135.YAMAZAKI, D., TRIGG, M. A. & IKESHIMA, D. 2015. Development of a global similar to 90 m water body map using multi-temporal Landsat images. *Remote Sensing of Environment,* 171**,** 337-351.YAMAZAKI, D., IKESHIMA, D., TAWATARI, R., YAMAGUCHI, T., O'LOUGHLIN, F., NEAL, J. C., SAMPSON, C. C., KANAE, S. & BATES, P. D. 2017. A high-accuracy map of global terrain elevations. *Geophysical Research Letters,* 44**,** 5844-5853.YAMAZAKI, D., IKESHIMA, D., SOSA, J., BATES, P. D., ALLEN, G. H. & PAVELSKY, T. M. 2019. MERIT Hydro: A High-Resolution Global Hydrography Map Based on Latest Topography Dataset. *Water Resources Research,* 55**,** 5053-5073.YUSOFF, I. M., RAMLI, A., ALKASIRAH, N. A. M., NASIR, N. A. A. M. J. G. M. J. O. S. & SPACE 2018. Exploring the managing of flood disaster: A Malaysian perspective. 14**,** 24-36.ZHOU, X., MA, W., ECHIZENYA, W. & YAMAZAKI, D. 2020. Uncertainty in flood frequency analysis of hydrodynamic model simulations. *Nat. Hazards Earth Syst. Sci. Discuss.,* 2020**,** 1-31.ZISCHG, A. P. & BERMÚDEZ, M. 2020. Mapping the Sensitivity of Population Exposure to Changes in Flood Magnitude: Prospective Application From Local to Global Scale. 8.